LETTER

doi:10.1038/nature14862

Protein synthesis by ribosomes with tethered subunits

Cédric Orelle[1]†*, Erik D. Carlson[2,3]*, Teresa Szal[1], Tanja Florin[1], Michael C. Jewett[2,3] & Alexander S. Mankin[1]

The ribosome is a ribonucleoprotein machine responsible for protein synthesis. In all kingdoms of life it is composed of two subunits, each built on its own ribosomal RNA (rRNA) scaffold. The independent but coordinated functions of the subunits, including their ability to associate at initiation, rotate during elongation, and dissociate after protein release, are an established model of protein synthesis. Furthermore, the bipartite nature of the ribosome is presumed to be essential for biogenesis, since dedicated assembly factors keep immature ribosomal subunits apart and prevent them from translation initiation[1]. Free exchange of the subunits limits the development of specialized orthogonal genetic systems that could be evolved for novel functions without interfering with native translation. Here we show that ribosomes with tethered and thus inseparable subunits (termed Ribo-T) are capable of successfully carrying out protein synthesis. By engineering a hybrid rRNA composed of both small and large subunit rRNA sequences, we produced a functional ribosome in which the subunits are covalently linked into a single entity by short RNA linkers. Notably, Ribo-T was not only functional *in vitro*, but was also able to support the growth of *Escherichia coli* cells even in the absence of wild-type ribosomes. We used Ribo-T to create the first fully orthogonal ribosome–messenger RNA system, and demonstrate its evolvability by selecting otherwise dominantly lethal rRNA mutations in the peptidyl transferase centre that facilitate the translation of a problematic protein sequence. Ribo-T can be used for exploring poorly understood functions of the ribosome, enabling orthogonal genetic systems, and engineering ribosomes with new functions.

The random exchange of ribosomal subunits between recurrent acts of protein biosynthesis presents an obstacle for making fully orthogonal ribosomes, a task with important implications for fundamental science, bioengineering, and synthetic biology. Previously, it was possible to redirect a subpopulation of the small ribosomal subunits from translating indigenous mRNAs to instead translating a specific mRNA by placing an alternative Shine–Dalgarno sequence in a reporter mRNA and introducing the complementary changes in the anti-Shine–Dalgarno region in 16S rRNA[2,3], which enabled selection of mutant 30S subunits with new decoding properties[4]. However, because large subunits freely exchange between native and orthogonal small subunits, creating a fully orthogonal ribosome has been impossible, thereby limiting the engineering of the 50S subunit, including the peptidyl transferase centre (PTC) and the nascent peptide exit tunnel, for specialized new properties.

The orthogonality of the full ribosome could be hypothetically achieved by linking the small and large subunit rRNA into a continuous molecule. A successful chimaeric 16S–23S construct must (1) properly interact with the ribosomal proteins and biogenesis factors for functional ribosome assembly; (2) avoid RNase degradation; and (3) have a linker(s) sufficiently short to ensure subunit *cis*-association, yet long enough for minimal interference with subunit movement required for translation initiation, elongation, and peptide release. In the native ribosome, the ends of 16S and 23S rRNA are too far apart (>170 Å) to be connected with a nuclease-resistant RNA linker. Therefore, we considered an alternative design in which the 23S rRNA would be 'grafted' into the 16S rRNA with the bridges connecting 16S and 23S rRNA sequences located across the rim of the subunits interface. To identify potential linking sites, we connected the native 23S rRNA ends that are proximal to each other, and generated new termini at different locations (Fig. 1a). This circular permutation approach has been successfully exploited *in vitro* previously[5], and a subsequent pilot study showed that three 23S rRNA circular permutation variants could assemble into a functional subunit *in vivo*[6]. We prepared a comprehensive collection of 91 circularly permutated 23S (CP23S) rRNA mutants with new ends placed at nearly every hairpin (Fig. 1b). The CP23S sequences were introduced in place of the wild-type 23S rRNA gene of the pAM552 plasmid (Fig. 1a, Extended Data Figs 1a and 2), and the resulting constructs were transformed in the *Escherichia coli* SQ171 cells lacking chromosomal rRNA alleles[7]. Twenty-two constructs were able to replace the resident plasmid pCSacB carrying the wild-type rRNA operon (Fig. 1b, Extended Data Fig. 2d, e and Extended Data Table 1). Most of the viable circularly permutated variants had new 23S rRNA ends at the subunit solvent side, including several locations close to the interface rim (Fig. 1c).

One of the viable mutants (CP2861, Fig. 1b) had 23S rRNA ends within the loop of helix 101 (H101), located in the ribosome near the apex loop of the 16S rRNA helix 44 (h44) (Figs 1c and 2c). Because the length of h44 varies among different species, and its terminal loop sequence can tolerate alterations[8], h44 was a promising site for grafting the CP2861 23S rRNA and generating a hybrid 16S–23S rRNA molecule (Fig. 2a–c). In the chimaeric rRNA, the processing sequences flanking the mature 16S rRNA would remain intact for proper maturation of the 16S rRNA termini, whereas endonuclease processing signals of 23S rRNA would be eliminated, thereby preventing its cleavage from the hybrid molecule.

The RNA linkers must span the 30–40 Å distance between h44 and H101 loops and allow for ~10 Å subunit ratcheting during protein synthesis[9–12] (Fig. 2c and Extended Data Fig. 3). Being unable to estimate the optimal length of the linkers accurately, we prepared a library of constructs, pRibo-T, in which the length of two tethers—T1 connecting 16S rRNA G1453 with 23S rRNA C2858, and T2 linking 23S C2857 with 16S G1454—varied from 7 to 12 adenine residues (Supplementary Table 2). Notably, plasmid exchange in SQ171 cells yielded several slowly growing colonies, and the pattern of extracted RNA showed a single major RNA species corresponding to the 16S–23S chimaera instead of the individual 16S and 23S bands (Fig. 2d). This result suggested that translation in these cells was carried out exclusively by Ribo-T, and revealed for the first time that the bipartite nature of the ribosome is dispensable for successful protein synthesis and cell viability.

[1]Center for Pharmaceutical Biotechnology – m/c 870, University of Illinois at Chicago, 900 South Ashland Avenue, Chicago, Illinois 60607, USA. [2]Department of Chemical and Biological Engineering, Northwestern University, 2145 Sheridan Road, Tech E-136, Evanston, Illinois 60208, USA. [3]Chemistry of Life Processes Institute, Northwestern University, 2170 Campus Drive, Evanston, Illinois 60208, USA. †Present address: Institut de Biologie et Chimie des Protéines, UMR5086 CNRS/Université Lyon 1, 7 passage du Vercors, 69367 Lyon, France.
*These authors contributed equally to this work.

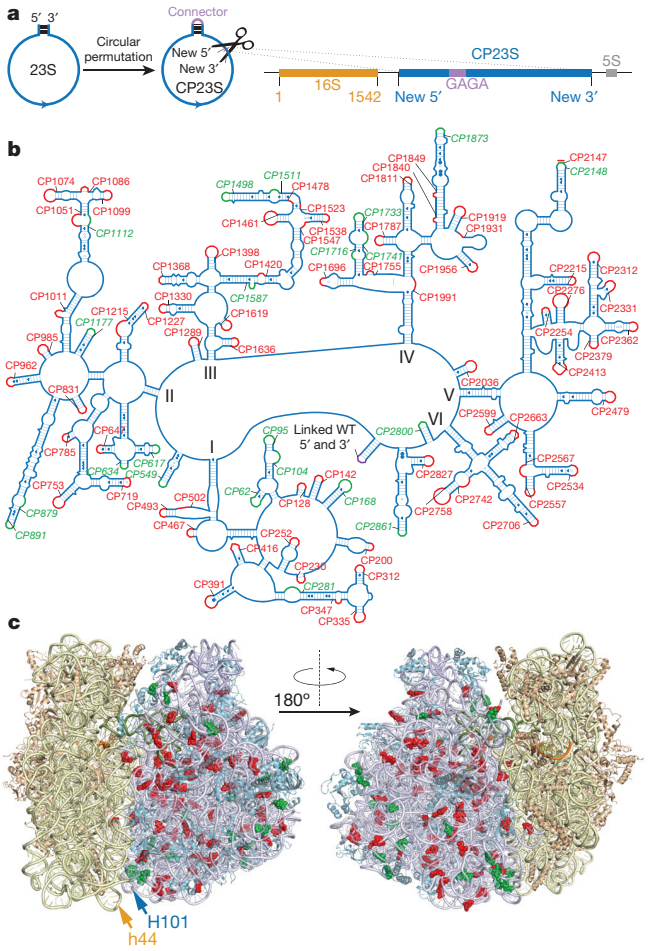

Figure 1 | Global screening of circularly permutated 23S rRNAs identifies variants capable of replacing the natural 23S rRNA in a functional ribosome. **a**, The general scheme for constructing the rRNA operon in which the mature 23S rRNA gene sequence is replaced with the circularly permutated gene (CP23S). **b**, Secondary structure diagram of 23S rRNA[26] showing circular permutation (CP) constructs tested for their ability to support cell growth in the absence of wild-type ribosomes, named according to the number of the new 5′ position in the wild-type (WT) 23S rRNA structure (for example, CP104). Viable circular permutation variants are green and italicized, non-viable variants are red. To assess the viability of CP mutants, two independent attempts to replace wild-type ribosomes with the CP construct were carried out. For all viable CP constructs, the lack of wild-type rRNA genes was confirmed by PCR as shown in the Extended Data Fig. 2, and the identity of the constructs in the resulting clones was verified by sequencing. **c**, The location of the new 5′ ends (spheres, viable in green, non-viable in red) of CP variants of the 23S rRNA in the crystallographic structure of the *E. coli* 70S ribosome[11] (Protein Data Bank (PDB) accession code 4V9D). The loops of helices h44 and H101 in the small and large subunit rRNA, respectively, used for subsequent experiments, are indicated by arrows.

The linker combinations 8A/9A or 9A/8A (for T1/T2) were found in the six best-growing clones. The first combination showed slightly better behaviour in some subsequent experiments and was chosen for further investigation (pRibo-T plasmid, Extended Data Fig. 1b). The original SQ171/pRibo-T clones, although viable, grew slowly (doubling time 107 ± 3 min compared to 35 ± 1 min for SQ171 cells expressing wild-type ribosomes), exhibited poor recovery from the stationary phase, and low cell density at saturation (Extended Data Fig. 4a). By passaging cells in liquid culture for approximately 100 generations, we isolated faster growing mutants. One such clone, SQ171fg/pRibo-T (for fast growing), exhibited better growth characteristics and shorter doubling time (70 ± 2 min) (Extended Data Fig. 4a). PCR and primer extension analysis showed the lack of wild-type rDNA and rRNA, respectively, confirming that every ribosome in this strain was assembled with the tethered rRNA (Extended Data Fig. 4b, c). Because the pRibo-T plasmid from the SQ171fg clone was unaltered, we sequenced the entire genome and found a nonsense mutation in the *ybeX* gene encoding a putative Mg^{2+}/Co^{2+} transporter, and a missense mutation in the *rpsA* gene encoding ribosomal protein S1 (Extended Data Fig. 4d, e). Either one of these mutations or their combined effect must account for the faster growth of SQ171fg/pRibo-T cells (henceforth called Ribo-T cells).

To establish that protein synthesis in Ribo-T cells was carried out by ribosomes with tethered subunits, we carefully examined the integrity of Ribo-T rRNA. Analysis of Ribo-T preparations in a denaturing gel showed only very faint 16S and 23S-like rRNA bands (marked by asterisks in Extended Data Fig. 5a), possibly reflecting the linker cleavage either in the cell or during Ribo-T isolation. In most of the multiple Ribo-T preparations, these cleavage products accounted for less than 4% of the total Ribo-T rRNA. In some of the preparations, these bands were completely absent (for example, lane 'Ribo-T(1)' in Extended Data Fig. 5a), showing that more than 99% of Ribo-T remained intact. Consistently, primer extension across the T1 and T2 linkers did not show any major stops attesting to the general stability of the oligo(A) connectors (Extended Data Fig. 5d). Protein synthesis rate in Ribo-T cells reached 50.5 ± 3.5% of that in cells with wild-type ribosomes (Extended Data Fig. 6a) and thus cannot be accounted for by a small fraction of Ribo-T with cleaved tethers. Unequivocal proof of active Ribo-T translation *in vivo* came from analysis of polysomes prepared from Ribo-T cells, in which intact 16S–23S hybrid rRNA (rather than the products of its cleavage) was associated with the heavy polysomal fractions (Fig. 2e). This result provided clear evidence that intact Ribo-T composed of covalently linked subunits is responsible for protein synthesis in the Ribo-T cells. 2D-gel analysis showed that most of the proteins present in SQ171 cells that express wild-type ribosomes are efficiently synthesized in the Ribo-T cells (Extended Data Fig. 6).

We isolated ribosomes with tethered subunits from Ribo-T cells and characterized their composition and properties. The tethered ribosome contains an apparently equimolar amount of 5S rRNA and the full complement of ribosomal proteins in quantities closely matching the composition of wild-type ribosome (Extended Data Fig. 5 b, c). Chemical probing showed that the rRNA hairpins h44 and H101 remain largely unperturbed, while both linkers were highly accessible to chemical modification, indicating that they are solvent-exposed (Extended Data Fig. 7).

Sucrose gradient analysis of Ribo-T showed that at 15 mM Mg^{2+} most of the ribosomal material sedimented as a 70S peak with a minor faster-sedimenting peak, which may represent Ribo-T dimers owing to cross-ribosome subunit association at a high Mg^{2+} concentration (Fig. 3a). At lower Mg^{2+} concentration (1.5 mM), when the native ribosome completely dissociates into subunits, Ribo-T still sediments as a single peak with an apparent sedimentation velocity of 65S (Fig. 3a). The distinctive resistance of Ribo-T to subunit dissociation offers a venue for isolating Ribo-T if it is expressed in cells concomitantly with wild-type ribosomes.

We then tested the activity of Ribo-T in the PURExpress *in vitro* translation system lacking native ribosomes[13]. Ribo-T efficiently synthesized the 18-kilodalton (kDa) dihydrofolate reductase or super folder green fluorescence protein (sfGFP)[14] (Fig. 3b). The rate of Ribo-T-catalysed protein synthesis reaches approximately 45% of that of the wild-type ribosomes (Fig. 3b). To assess which translation step is the most problematic for Ribo-T, progression of Ribo-T through a short synthetic gene[15] was analysed by toe-printing (Fig. 3c). A more pronounced band of the ribosomes at the open reading frame start codon indicated that Ribo-T is impaired in translation initiation at a step subsequent to the start codon recognition. Although the true nature of this effect will require further investigation, it is unlikely to reflect a lower affinity of Ribo-T for initiation factors because higher concentrations of IF1, IF2 and IF3 could not rescue the initiation defect (data not shown).

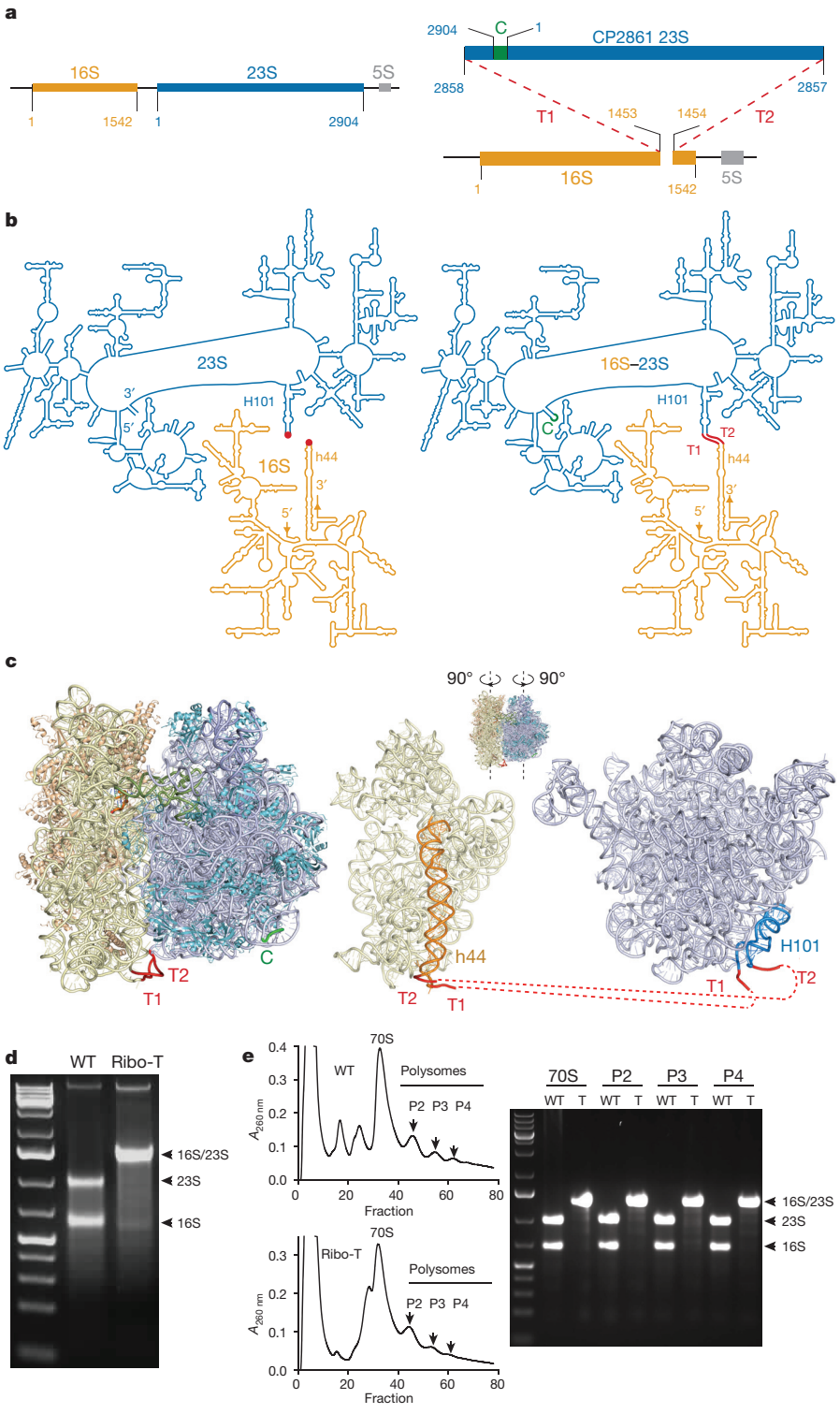

Figure 2 | Ribo-T design. **a**, Wild-type (left) and Ribo-T (right) rRNA genes. In Ribo-T, the circularly permutated 23S rRNA gene, 'closed' at its native ends with a four-nucleotide long connector (C) and 'opened' in the loop of H101, is inserted via short tethers T1 and T2 into the apex loop of h44 in the 16S rRNA gene. The resulting hybrid rRNA gene is transcribed as a single chimaeric 16S–23S rRNA, with its 5′ and 3′ ends probably processed by the enzymes of 16S rRNA maturation. **b**, Secondary structure of the mature wild-type (left) and Ribo-T (right) rRNAs. The red dots indicate the apex loops of h44 and H101, which in Ribo-T are connected by tethers T1 and T2. The arrows at the 16S rRNA ends and the tethers in the Ribo-T map indicate the direction of transcription of the chimaeric 16S–23S rRNA. **c**, Left, the locations of the T1 and T2 tethers in the three-dimensional model of Ribo-T (based on the structure of *E. coli* ribosome in the unrotated state[11]; PDB code 4V9D). 16S rRNA is in yellow, 30S proteins are in orange, 23S and 5S rRNA are in blue, 50S proteins are in cyan, P-site-bound tRNA is in olive, mRNA is in orange, connector (C) linking 23S native 5′ and 3′ ends is in green, and tethers T1 and T2 are in red. Right, the ribosome has been opened up like a book, exposing the subunit interface, with helices h44 (16S) and H101 (23S) highlighted in orange and blue, respectively, and ribosomal proteins removed for clarity. **d**, Agarose gel electrophoresis of total RNA prepared from SQ171 cells expressing wild-type ribosomes or Ribo-T. The gel is representative of five independent biological replicates. **e**, Left, sucrose gradient fractionation of polysomes prepared from cells expressing wild-type ribosomes (top) or Ribo-T (bottom). Peaks corresponding to monosomes (70S), disomes (P2), trisomes (P3) and tetrasomes (P4) are indicated by arrows. Right, the agarose electrophoresis analysis of RNA extracted from the corresponding sucrose gradient peaks, wild-type ribosomes (WT) or Ribo-T (T).

To enable a fully orthogonal ribosome–mRNA system, we next engineered a Ribo-T version (oRibo-T) committed to translation of a particular orthogonal cellular mRNA. The wild-type 16S anti-Shine–Dalgarno region was altered from ACCUCCUUA to AUUGUGGUA (ref. 3) producing a poRibo-T1 construct. When poRibo-T1 was introduced in *E. coli* carrying the *sf-gfp* gene with the Shine–Dalgarno sequence CACCAC cognate to oRibo-T (Extended Data Fig. 1c, pLpp5oGFP), notable sfGFP expression was observed (Extended Data Fig. 8a), demonstrating the activity of oRibo-T.

Ribosomes prepared from poRibo-T1-transformed cells (containing a mixture of wild-type ribosomes and oRibo-T) translated an orthogonal *sf-gfp* gene in a cell-free system (green dotted line in Extended Data Fig. 8b). However, because the orthogonal *sf-gfp* transcript is the only mRNA available during *in vitro* translation and no native mRNA engage wild-type 30S subunits, a fraction of orthogonal sfGFP biosynthesis is accounted for by wild-type ribosomes (pink dotted line in Extended Data Fig. 8b). Therefore, to isolate oRibo-T1 activity *in vitro*, we used the A2058G mutation in the 23S rRNA portion of oRibo-T, which rendered

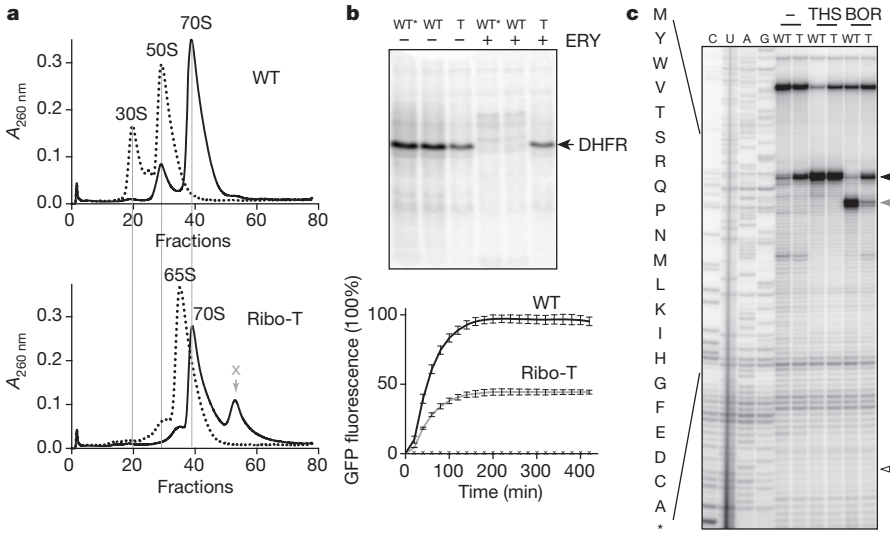

Figure 3 | Functional characterization of Ribo-T. **a**, Sucrose gradient analysis of wild-type ribosomes (top) and Ribo-T (bottom) under 15 mM $MgCl_2$ (solid line) or 1.5 mM $MgCl_2$ subunit dissociating conditions (dotted line). The peak marked with grey arrow and 'X' may represent Ribo-T dimers. The result was qualitatively verified in an independent experiment performed at Mg^{2+} concentrations 1.5 mM and 10 mM. **b**, *In vitro* translation of proteins by isolated Ribo-T. Top, SDS–PAGE analysis of the dihydrofolate reductase (DHFR) protein synthesized in the Δribosome PURExpress system supplemented with purified wild-type ribosomes or Ribo-T (T); wild-type ribosomes provided with the kit (WT*) were used as a control. The transcription–translation reaction was carried out in the presence of [^{35}S]L-methionine in the absence or presence of 50 μM erythromycin (ERY). The A2058G mutation in Ribo-T renders the Ribo-T-driven translation resistant to the antibiotic. The 'no erythromycin' samples are a representative result of two independent biological experiments. Bottom, time course of sfGFP protein expression in the Δribosome PURExpress system supplemented with purified wild-type (black) or Ribo-T (grey) ribosomes. The k_{obs} rates (385 ± 13 relative fluorescent units (RFU) min^{-1} (mean ± s.d.) for wild-type, 177 ± 6 RFU min^{-1} for RiboT) were determined from the initial slopes. The activity of both ribosomes was fully inhibited by 50 μg ml^{-1} chloramphenicol (time points indicated by x). Each curve is an average of two independent biological replicates, with error bars indicating the s.d. **c**, Toeprinting analysis of translation of a 20-codon synthetic gene *RST1* (ref. 15) by wild-type ribosomes or Ribo-T. The antibiotic thiostrepton (THS), present at 50 μM, arrests the initiating ribosome at the start codon[19] (black arrowhead). The threonyl-tRNA synthetase inhibitor borrelidin (BOR) arrests translation at the fourth codon of *RST1* mRNA (grey arrowhead)[15]. The position of a toeprint band that would correspond to the ribosome that has reached the RST1 stop codon is shown by an open arrowhead. A more pronounced toeprint band at the start codon in the samples lacking thiostrepton indicates that Ribo-T departs from the initiation codon slower than wild-type ribosomes. A weaker borrelidin-specific band observed in the Ribo-T sample suggests that under our experimental conditions, fewer Ribo-T compared to wild-type ribosomes were able to reach the fifth codon, apparently owing to slower initiation.

ribosomes resistant to macrolide and lincosamide antibiotics (for example, clindamycin). The addition of clindamycin to the reaction with wild-type ribosomes completely inhibited expression of the reporter (pink solid line in Extended Data Fig. 8b), whereas marked sfGFP expression was observed in the reaction carrying the oRibo-T preparation (green solid line in Extended Data Fig. 8b). Importantly, the unique conjoined nature of Ribo-T allows for using antibiotic-resistance mutations in any of the ribosomal subunits. We demonstrated this by introducing a G693A mutation in the small subunit moiety of oRibo-T, rendering oRibo-T resistant to pactamycin[16,17]. Pactamycin (100 μM) completely inhibited the activity of the wild-type ribosomes in the PURExpress translation system, whereas oRibo-T(G693A) remained fully active (Extended Data Fig. 8c).The combination of an orthogonal translation initiation signal with the antibiotic-resistance mutations embedded in oRibo-T allows for exploring unique properties of oRibo-T in a cell-free system even in preparations carrying a substantial fraction of wild-type ribosomes.

During subsequent experiments, we fortuitously isolated a mutant version of the poRibo-T1 plasmid (poRibo-T2) that contained a single mutation in the P_L promoter that improved its transformation properties and was used thereafter (Extended Data Fig. 9).

We next demonstrated the evolvability of oRibo-T by selecting the gain-of-function mutations in the PTC, which could facilitate translation of a problematic protein sequence by the ribosome. The SecM polypeptide presents a classic example of an amino acid sequence for which translation is problematic for the ribosome[18]. The expression of the essential SecA secretion ATPase is controlled by programmed ribosome stalling at the Pro166 codon of *secM*. Translation arrest ensues because specific interactions of the SecM nascent chain with the ribosomal exit tunnel impair the PTC function, preventing the transfer of the 165-amino-acid long peptide to the incoming prolyl-transfer-RNA (Pro-tRNA). Several mutations in the ribosomal exit tunnel (for example, A2058G) have been previously identified as relieving translation arrest possibly by disrupting the interactions between the nascent chain and ribosome, and rRNA residues in the PTC A-site have been proposed to have a key role in the mechanism of ribosome stalling[18–20]. However, exploring the role of the PTC in the mechanism of the translation arrest has been impossible so far because of the lethal nature of PTC mutations[21,22].

We therefore asked whether the PTC A-site mutations can relieve SecM-induced translation arrest. Our interest in testing the use of oRibo-T for manipulating the ribosomal A-site was additionally fuelled by future prospects of engineering ribosomes capable of programmed polymerization of unnatural amino acids and backbone-modified analogues. To search for SecM arrest bypass mutations, we removed the A2058G mutation from poRibo-T2 and prepared a library of plasmids with mutations at two 23S residues, A2451 and C2452. These residues form the amino acid binding pocket in the PTC A-site[10,23] (Fig. 4b), and their mutations are dominantly lethal in *E. coli*[21,22]. We also engineered an orthogonal SecM-based reporter, poSML (Fig. 4a and Extended Data Fig. 1d), encoding the SecM arrest sequence fused in frame with *lacZa* gene[18] (Fig. 4a).

Notably, when the C41(DE3) cells capable of α-complementation were transformed first with the poSML reporter and then with the poRibo-T2(A2451N/C2452N) mutant library, some of the colonies gained blue colour on indicator plates (Fig. 4c), demonstrating read-through of the SecM arrest sequence in some of the mutants. Sequencing 15 bluer colonies showed that they all carried a C2451–

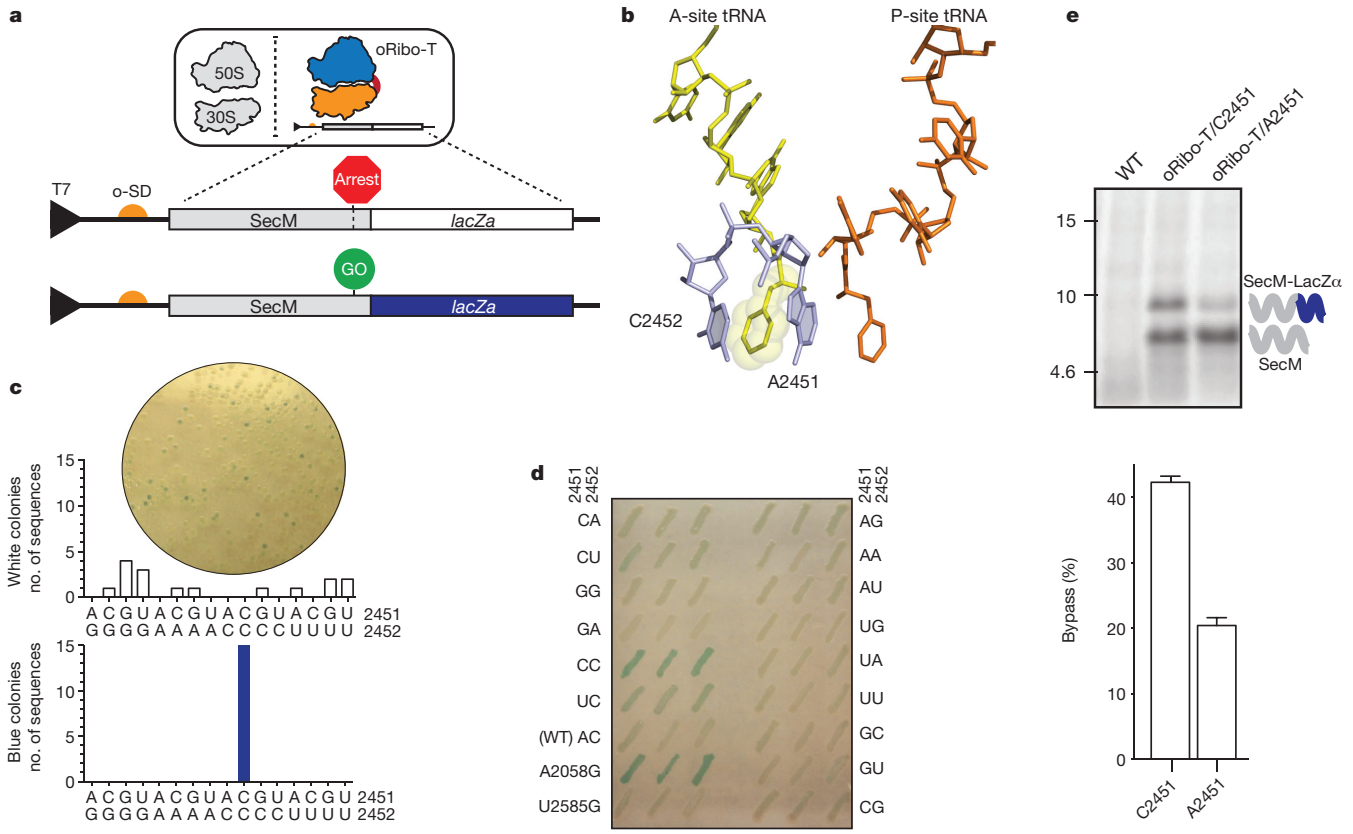

Figure 4 | Evolving Ribo-T to identify gain-of-function PTC mutations that facilitate synthesis of problematic amino acid sequences. **a**, The SecM-LacZα reporter with an orthogonal Shine–Dalgarno (o-SD) sequence is translated in the cell by oRibo-T. SecM-dependent ribosome stalling prevents expression of the *lacZa* gene unless a ribosomal mutation allows for bypass of the SecM arrest site. **b**, The placement of Phe-tRNAs bound in the P-site (orange) and A-site (yellow) of the PTC[10]. The conserved 23S rRNA residues A2451 and C2452 (blue) form the amino acid side-chain binding pocket in the A-site. **c**, Top, colonies formed on X-gal/isopropyl β-D-1-thiogalactopyranoside (IPTG) plates by the *E. coli* C41 cells transformed with the *secM-lacZa* reporter plasmid and a library of poRibo-T2 plasmids with the PTC mutations at positions 2451 and 2452. Bottom, identity of 2451 and 2452 residues in poRibo-T2 plasmids isolated from randomly picked 16 white colonies and 15 blue colonies. **d**, The *E. coli* C41 cells transformed with the *secM-lacZa* reporter and individual poRibo-T2 plasmids with different nucleotide combinations at positions 2451 and 2452. The transformed cells were initially plated on LB agar antibiotic plate without X-gal or IPTG (all colonies pale), and three randomly picked transformants were then streaked on the shown indicator plate containing X-gal and IPTG. The poRibo-T2 mutant with the A2058G mutation, which is known to enhance the bypass of the SecM arrest sequence[18], was used as a positive control. A mutation of another essential PTC nucleotide (U2585G), which has been proposed to be implicated in some translation arrest scenarios[27], showed no effect on SecM arrest. The photographs of the agar plates in **c** and **d** have been contrast-enhanced for better colour separation. **e**, The A2451C mutation enhances bypass of the SecM stalling sequence by oRibo-T *in vitro*. The orthogonal construct containing *secM* stalling sequence fused in frame to the truncated *lacZa* gene was translated in the ΔRibosome PURExpress cell-free translation system supplemented with wild-type non-tethered ribosomes or preparations of oRibo-T (A2451 or C2451). The Ribo-T constructs carried the pactamycin-resistance mutation G693A in 16S rRNA, and the reactions were carried out in the presence of pactamycin, which, in addition to the presence of an orthogonal Shine–Dalgarno sequence, ensured that the reporter is translated exclusively by oRibo-T (see the control wild-type lane with no translation products). Numbers on the left indicate the size (kDa) of molecular mass markers. The bar graph at the bottom shows the efficiency of bypass (ratio between the full-size and SecM-arrested translation products). A representative gel of two independent experiments is shown, with error bars indicating the s.d.

C2452 sequence (the A2451C mutation) in the PTC. By contrast, none of the 16 analysed 'white' colonies had this sequence, and instead exhibited a variety of dinucleotide combinations at positions 2451–2452 (Fig. 4c). We corroborated these results by individually testing all possible 2451–2452 mutants in poSML-transformed C41(DE3) cells. Importantly, all the mutants were viable, confirming that oRibo-T is suitable for expression of dominantly lethal 23S rRNA mutations *in vivo*, indicating a low degree of cross-association of oRibo-T with free wild-type 30S subunits. Consistent with our previous result (Fig. 4c), the A2451C mutation confers the most pronounced blue colour of the transformants, comparable to that seen in cells expressing oRibo-T with the tunnel mutation A2058G (Fig. 4d). The A2451U mutation also increased the blue hue of the cells although to a lesser extent. These results suggested that the A2451C (and A2451U) mutants were not only functional in cellular protein synthesis but also gained the ability to bypass translation arrest caused by the SecM sequence.

We verified *in vitro* the discovered role of A2451 in the mechanism of SecM translation arrest by testing the translation of the orthogonal *secM-lacZa* gene by isolated oRibo-T with and without the A2451C mutation. To assure oRibo-T activity only, the pactamycin-resistance mutation G693A (refs 16, 17) was introduced into the 16S segment of oRibo-T constructs, and cell-free translation in the PURExpress system was carried out in the presence of pactamycin. Only a small fraction of original oRibo-T was able to bypass the SecM arrest signal and synthesize the full-size hybrid protein (Fig. 4e, lane oRibo-T/A2451). By contrast, the A2451C mutant was able to bypass the SecM arrest site twice as efficiently as the unmodified oRibo-T (Fig. 4e, lane oRibo-T/C2451), confirming that the selected (and otherwise lethal) mutation in the PTC has improved the ability of oRibo-T

to polymerize a polypeptide sequence problematic for wild-type ribosomes. These results provide the first, to our knowledge, direct experimental evidence of a direct involvement of the PTC A-site in the mechanism of nascent peptide-dependent ribosome stalling, and suggest that interactions between the proline moiety of Pro-tRNA and the A-site rRNA residues are crucial for the SecM-induced translation arrest.

By engineering a ribosome with inseparable tethered subunits, and demonstrating its functionality *in vivo* and *in vitro*, we have revised one of the key concepts of molecular biology: that successful expression of the genome requires reversible association and dissociation of the ribosome into individual subunits. Although the ability of translation initiation by 70S ribosome at leaderless mRNAs or via scanning re-initiation has been previously demonstrated[24,25], it was surprising that Ribo-T would be active enough to express the entire bacterial genome at a sufficient level for active cell growth and proliferation. This finding in turn made possible a fully orthogonal and evolvable gene expression system in the cell in which an entire specialized ribosome, not just the mRNA-interacting small subunit, is dedicated to the translation of a defined genetic template. As a proof of principle we showed that oRibo-T can be used for studying in cells mutations of functionally crucial rRNA residues that are dominantly lethal, a task that would be difficult or impossible to achieve in any other system. This shows that Ribo-T may find important implications in exploring poorly understood functions of the ribosome in protein synthesis. Furthermore, the opportunity provided by the oRibo-T system to modify the catalytic properties of the protein synthesis machine opens up exciting prospects for engineered ribosomes with principally new properties.

Online Content Methods, along with any additional Extended Data display items and Source Data, are available in the online version of the paper; references unique to these sections appear only in the online paper.

Received 28 January; accepted 26 June 2015.
Published online 29 July 2015.

1. Karbstein, K. Quality control mechanisms during ribosome maturation. *Trends Cell Biol.* **23,** 242–250 (2013).
2. Hui, A. & de Boer, H. A. Specialized ribosome system: preferential translation of a single mRNA species by a subpopulation of mutated ribosomes in *Escherichia coli*. *Proc. Natl Acad. Sci. USA* **84,** 4762–4766 (1987).
3. Rackham, O. & Chin, J. W. A network of orthogonal ribosome·mRNA pairs. *Nature Chem. Biol.* **1,** 159–166 (2005).
4. Neumann, H., Wang, K., Davis, L., Garcia-Alai, M. & Chin, J. W. Encoding multiple unnatural amino acids via evolution of a quadruplet-decoding ribosome. *Nature* **464,** 441–444 (2010).
5. Erlacher, M. D. *et al.* Chemical engineering of the peptidyl transferase center reveals an important role of the 2′-hydroxyl group of A2451. *Nucleic Acids Res.* **33,** 1618–1627 (2005).
6. Kitahara, K. & Suzuki, T. The ordered transcription of RNA domains is not essential for ribosome biogenesis in *Escherichia coli*. *Mol. Cell* **34,** 760–766 (2009).
7. Asai, T., Zaporojets, D., Squires, C. & Squires, C. L. An *Escherichia coli* strain with all chromosomal rRNA operons inactivated: complete exchange of rRNA genes between bacteria. *Proc. Natl Acad. Sci. USA* **96,** 1971–1976 (1999).
8. Dorywalska, M. *et al.* Site-specific labeling of the ribosome for single-molecule spectroscopy. *Nucleic Acids Res.* **33,** 182–189 (2005).
9. Yusupov, M. M. *et al.* Crystal structure of the ribosome at 5.5 Å resolution. *Science* **292,** 883–896 (2001).
10. Voorhees, R. M., Weixlbaumer, A., Loakes, D., Kelley, A. C. & Ramakrishnan, V. Insights into substrate stabilization from snapshots of the peptidyl transferase center of the intact 70S ribosome. *Nature Struct. Mol. Biol.* **16,** 528–533 (2009).
11. Dunkle, J. A. *et al.* Structures of the bacterial ribosome in classical and hybrid states of tRNA binding. *Science* **332,** 981–984 (2011).
12. Frank, J. & Agrawal, R. K. A ratchet-like inter-subunit reorganization of the ribosome during translocation. *Nature* **406,** 318–322 (2000).
13. Shimizu, Y. *et al.* Cell-free translation reconstituted with purified components. *Nature Biotechnol.* **19,** 751–755 (2001).
14. Pédelacq, J. D., Cabantous, S., Tran, T., Terwilliger, T. C. & Waldo, G. S. Engineering and characterization of a superfolder green fluorescent protein. *Nature Biotechnol.* **24,** 79–88 (2006).
15. Orelle, C. *et al.* Identifying the targets of aminoacyl-tRNA synthetase inhibitors by primer extension inhibition. *Nucleic Acids Res.* **41,** e144 (2013).
16. Mankin, A. S. Pactamycin resistance mutations in functional sites of 16S rRNA. *J. Mol. Biol.* **274,** 8–15 (1997).
17. Orelle, C. *et al.* Tools for characterizing bacterial protein synthesis inhibitors. *Antimicrob. Agents Chemother.* **57,** 5994–6004 (2013).
18. Nakatogawa, H. & Ito, K. The ribosomal exit tunnel functions as a discriminating gate. *Cell* **108,** 629–636 (2002).
19. Vázquez-Laslop, N., Ramu, H., Klepacki, D., Ci, K. & Mankin, A. S. The key role of a conserved and modified rRNA residue in the ribosomal response to the nascent peptide. *EMBO J.* **29,** 3108–3117 (2010).
20. Bhushan, S. *et al.* SecM-stalled ribosomes adopt an altered geometry at the peptidyl transferase center. *PLoS Biol.* **9,** e1000581 (2011).
21. Thompson, J. *et al.* Analysis of mutations at residues A2451 and G2447 of 23S rRNA in the peptidyltransferase active site of the 50S ribosomal subunit. *Proc. Natl Acad. Sci. USA* **98,** 9002–9007 (2001).
22. Sato, N. S., Hirabayashi, N., Agmon, I., Yonath, A. & Suzuki, T. Comprehensive genetic selection revealed essential bases in the peptidyl-transferase center. *Proc. Natl Acad. Sci. USA* **103,** 15386–15391 (2006).
23. Nissen, P., Hansen, J., Ban, N., Moore, P. B. & Steitz, T. A. The structural basis of ribosome activity in peptide bond synthesis. *Science* **289,** 920–930 (2000).
24. Moll, I., Hirokawa, G., Kiel, M. C., Kaji, A. & Blasi, U. Translation initiation with 70S ribosomes: an alternative pathway for leaderless mRNAs. *Nucleic Acids Res.* **32,** 3354–3363 (2004).
25. Karamyshev, A. L., Karamysheva, Z. N., Yamami, T., Ito, K. & Nakamura, Y. Transient idling of postermination ribosomes ready to reinitiate protein synthesis. *Biochimie* **86,** 933–938 (2004).
26. Cannone, J. J. *et al.* The Comparative RNA Web (CRW) Site: an online database of comparative sequence and structure information for ribosomal, intron, and other RNAs. *BMC Bioinformatics* **3,** 2 (2002).
27. Arenz, S. *et al.* Molecular basis for erythromycin-dependent ribosome stalling during translation of the ErmBL leader peptide. *Nat. Commun.* **5,** 3501 (2014).

Supplementary Information is available in the online version of the paper.

Acknowledgements We thank I. Ntai for mass spectrometry analysis, K. N. Swonger, C. Burghard, E. M. Fulk, V. Raghavan and N. Aleksashin for help with some experiments, K. Ito for providing the sequence of the pNH122 *secM-lacZa* reporter, Y. Polikanov for help in preparing ribosome images, J. Lee for assistance in genome sequence analysis, S. Sothiselvam and J. Marks for discussions and suggestions, and N. Vazquez-Laslop for advice on the project and critical reading of the manuscript. This work was supported by the Defense Advanced Research Projects Agency (N66001-12-C-4211), the National Science Foundation grants MCB-0943393 (to M.C.J.) and MCB-1244455 (to A.S.M.) and the David and Lucille Packard Foundation Fellowship (2011-37152) (to M.C.J.).

Author Contributions M.C.J. and A.S.M. designed the study, analysed results, and wrote the paper. C.O. and E.D.C. designed and performed experiments and analysed data. T.S. and T.F. performed experiments.

Author Information Reprints and permissions information is available at www.nature.com/reprints. The authors declare no competing financial interests. Readers are welcome to comment on the online version of the paper. Correspondence and requests for materials should be addressed to A.S.M. (shura@uic.edu) or M.C.J. (m-jewett@northwestern.edu).

METHODS

No statistical methods were used to predetermine sample size.

Preparation of circularly permuted variants of the 23S rRNA. The A2058G mutation was introduced into the pAM552 plasmid (Extended Data Fig. 1a) by inverse PCR using primers 5′-CCGTCTTGCCGCGGGTAC-3′ and 5′-GTGTACCCGCGGCAAGACGG***G***AAGACCCCGTGAACC-3′ (the underlined sequence is complementary to the second primer and the mutation is shown by italicized bold character) followed by re-circularization by Gibson assembly reaction[28] (all primers used in this study were synthesized by Integrated DNA Technology). A 23S-A2058G gene with native 5′ and 3′ ends linked by a GAGA tetra-loop was generated by inverse PCR using primers 5′-GGTTAAGCCTCACGGTTC-3′ and 5′-CCGTGAGGCTTAACC**GAGA**GGTTAAGCGACTAAGCGTAC-3′ (GAGA tetra loop in bold) and pAM552-A2058G as template. Purified PCR product (50 ng) was circularized by Gibson assembly reaction for 1 h at 50 °C. The resulting circular 23S rRNA gene was then cloned at its native unique EagI restriction site (position 1905 in wild-type 23S rRNA gene) into T7-Flag-4 plasmid (Sigma Aldrich) as follows. The circularized 23S rRNA gene was amplified by inverse PCR using primers 5′-GAGACACAACGTGGCTTTCCGGCCGTAACTATAACG-3′ and 5′-CACTCGTCGAGATCGATCTTCGGCCGCCGTTTACC-3′ (added homology to the T7-Flag-4 vector underlined) and Gibson-assembled with the T7-Flag-4 vector amplified with the primers 5′-AAGATCGATCTCGACGAGTG-3′ and 5′-GAAAGCCACGTTGTGTCTC-3′. The cloned circularly permuted 23S rRNA gene in the resulting plasmid pCP23S-EagI containing a pBR322 origin of replication and KanR selective marker (Extended Data Fig. 2) was fully sequenced.

The pCP23S-EagI plasmid was then digested with EagI (New England Biolabs) for 1 h at 37 °C, and the circularly permutated 23S rRNA (CP23S) gene was isolated from a SYBRSafe-stained 0.7% agarose gel using a E.Z.N.A. Gel Extraction kit (Omega). The 23S rRNA was circularized by T4 DNA ligase (New England Biolabs) in a 50 µl reaction with 2.5 ng µl^{-1} DNA for 14 h at 16 °C, followed by heat inactivation at 65 °C for 10 min. The reaction was diluted 1:100 for use as a template in the PCR reactions for generating the circular permutants (Extended Data Fig. 2).

Ninety-one CP23S mutants were designed by introducing new 23S rRNA 5′ and 3′ ends at most of the apex loops and some internal loops of rRNA helices to assure spatial proximity of the new rRNA termini in the fully assembled 50S ribosomal subunit. Each CP23S rRNA gene was PCR-amplified in a 40 µl reaction using Phusion High Fidelity DNA polymerase (New England Biolabs), with primer pairs shown in Supplementary Table 1, and 4 µl of the 1:100 diluted 23S circular ligation reaction as template. Each primer pair adds to the 5′ and 3′ ends of the amplified CP23S gene 20-base-pair (bp) of homology to the 23S rRNA processing stem retained in the target vector pAM552-Δ23S-AflII (described below). PCR reactions catalysed by the Phusion High Fidelity DNA polymerase were run under the following conditions: 98 °C, 10 min followed by 25 cycles (98 °C, 30 s; 60 °C, 30 s; 72 °C, 180 s), followed by the final incubation for 15 min at 72 °C. The reaction product was purified using E.Z.N.A. Cycle Pure kit (Omega) and the size of the amplified DNA was confirmed by electrophoresis in a 1% agarose gel. For circular permutations with off target bands (12 in total), the PCR product of the correct size was extracted from the agarose gel.

To minimize PCR errors in generating the vector backbone, which carried 16S and 5S rRNA sequences, and prevent carry-through of the wild-type *rrnB* operon, universal backbone vector pAM552-Δ23S-AflII lacking the 23S rRNA gene and containing added AflII restriction site for cloning of CP23S was prepared. The plasmid pAM552-AflII was constructed from pAM552 by adding AflII restriction sites within the terminal stem of the wild-type 23S rRNA gene by introducing the G2C and C2901G mutations. First, the G2C mutation was introduced by inverse PCR using 5′-phosphorylated primers **C**TTAAGCGACTAAGCGTACAC and CTCACAACCCGAAGATGTTTC, followed by blunt-end ligation, transformation into *E. coli* POP2136 electrocompetent cells, plating on LB-agar plates supplemented with 50 µg ml^{-1} carbenicillin, growth overnight at 30 °C, single colony isolation and sequencing. The C2901G mutation was added by the same method using 5′-phosphorylated primers **G**CTTACAACGCCGAAGCTG and TTAAGCCTCACGGTTCATTAG. The introduced mutations preserved the integrity of the 23S rRNA terminal stem and did not affect growth of SQ171 cells expressing only ribosomes with the pAM552-AflII-encoded rRNA (doubling times 53.9 ± 1.0 min for SQ171 cells transformed with pAM552 and 53.3 ± 2.4 min for SQ171 transformed with pAM552-AflII, as determined from four separate colonies each on Biotek Synergy H1 plate readers in 96-well flat bottom plates (Costar) in 100 µl LB supplemented with 50 µg ml^{-1} carbenicillin, 37 °C, linear shaking with 2 mm amplitude, at 731 cycles per min). To remove the 23S rRNA gene, pAM552-AflII was digested with AflII (New England Biolabs) for 1 h at 37 °C, the backbone portion of the vector was gel-purified and ligated with T4 DNA ligase (New England Biolabs) overnight at 16 °C. It was then transformed into POP2136 cells, plated on LB/agar plates supplemented with 50 µg ml^{-1} carbenicillin, and grown at 30 °C. Plasmids from several colonies were isolated and fully sequenced. The resulting pAM552-Δ23S-AflII plasmid contains the 16S rRNA, 23S processing stems with an added AflII restriction site, 5S rRNA, and β-lactamase resistance gene and ColE1 ori (Extended Data Fig. 2). Vector backbone was prepared by digesting pAM552-Δ23S-AflII with AflII restriction enzyme at 37 °C for 2 h and purification using an E.Z.N.A. Cycle Pure kit.

All the CP23S constructs were assembled in parallel by Gibson assembly reaction (Extended Data Fig. 2) in a 96-well PCR plate. For each CP23S target, 50 ng of AflII-digested purified backbone was added to threefold molar excess of the PCR-amplified and purified CP23S insert. Gibson assembly mix[28] (15 µl) was added, the final volumes brought to 48 µl with nuclease-free water, and incubated at 50 °C for 1 h in the PCR machine. No CP23S insert was added to the negative control reaction. To check the efficiency of DNA assembly, 2 µl of selected assembly reactions were transformed into electrocompetent POP2136 cells. After 1 h recovery at 37 °C in SOC media, a quarter of each transformation was plated on LB-agar plates supplemented with 50 µg ml^{-1} carbenicillin and grown for 20 h at 30 °C. A typical CP23S assembly reaction generated 30–120 POP2136 colonies with the control reaction generating only few colonies.

Testing CP23S rRNA constructs. Transformation of SQ171/pCSacB rubidium chloride-competent cells was carried out in a 96-well plate. Two microlitres of the Gibson Assembly reactions were added to 20 µl competent cells in the pre-chilled plate. After a 45-min incubation in ice/water bath, 45 s at 42 °C and 2 min on ice, 130 µl of SOC medium was added to the wells and the plate was incubated 2 h at 37 °C with shaking at 600 r.p.m. on a microplate shaker. Forty microlitres of medium were then transferred from each well to the wells of another 96-well plate containing 120 µl SOC supplemented with 100 µg ml^{-1} ampicillin and 0.25% sucrose. The plate was incubated overnight at 37 °C with shaking at 600 r.p.m. A 96-pin replicator was used to spot aliquots of the cultures onto a rectangular LB agar plate containing 100 µg ml^{-1} ampicillin, 5% sucrose and 1 mg ml^{-1} erythromycin. The plate was incubated overnight at 37 °C and the appearance of Amp^r/Ery^r transformants was recorded. The completeness of the replacement of the wild-type pCSacB plasmid with the plasmids carrying circularly permutated 23S rRNA gene was verified by PCR using a mixture of three primers: primer 1 (5′-GCAGATTAGCACGTCCTTCA-3′) complementary to the 23S rRNA segment 50–69), primer 2 (5′-CGTTGAGCTAACCGGTACTA-3′) containing the sequence of the 23S rRNA segment 2863–2882, and primer 3 (5′-GGGTGATGTTTGAGATATTTGCT-3′) corresponding to the sequence of the 16S/23S intergenic spacer 139–116 bp upstream from the 23S rRNA gene in *rrnB* (Extended Data Fig. 2e). The combination of the primers 1 and 3 produces a 207-bp PCR band if the wild-type *rrn* operon is present; the combination of primers 1 and 2 produces a 112-bp PCR band on the templates with circularly permutated 23S rRNA gene (Extended Data Fig. 2e).

To reduce the number of false-negative CP23S rRNA variants, the experiment was repeated one more time using *de novo* assembled Gibson reactions with the cp23S rRNA constructs that failed to replace pCSacB in the first experiment. Two additional functional CP23S rRNA constructs were recovered from the second attempt. Altogether, 22 CP23S rRNA variants were able to replace pCSacB in the SQ171 cells. CP23S identity was confirmed by plasmid sequencing. Growth rates were analysed on Biotek Synergy H1 plate readers in 96-well flat bottom plates (Costar) in 100 µl LB with 50 µg ml^{-1} carbenicillin. Doubling times and final $A_{600\ nm}$ after 18 h are shown in Extended Data Table 1.

Construction of pRibo-T. To avoid generation of mutations in the 23S rRNA gene during PCR amplification for Gibson assembly, the 23S rRNA gene variant circularly permuted at H101 (corresponding to CP2861 from Fig. 1) was first cloned in the pUC18 vector. For that, the 23S rRNA gene circularly permuted at H101 was PCR-amplified from circularized 23S rRNA gene prepared in the circular permutation study (see above and Extended Data Fig. 2a) by using the high-fidelity AccuPrime Taq polymerase (Life Technologies) and primers containing BamHI restriction sites (shown in bold) 5′-TATT**GGATCC**GATGCGTTGAGCTAACCGGTA-3′ and 5′-TTAT**GGATCC**TGCGCTTACACACCCGGCCTAT-3′. The amplified fragment was cut with BamHI and cloned in dephosphorylated BamHI-cut pUC18 plasmid. A plasmid containing CP2861 23S rRNA (pUC23S) was fully sequenced to verify the lack of mutations in the 23S rRNA gene.

For preparation of pRibo-T (Extended Data Fig. 1b), pAM552-Δ23S-AflII plasmid (see above) served as a recipient for the CP2861 23S rRNA gene. The CP2861 23S RNA gene was excised from the pUC23S plasmid by BamHI digestion and gel purified. To graft the CP2861 23S rRNA gene into the 16S rRNA gene, the plasmid backbone was prepared by PCR-amplifying the plasmid pAM552-Δ23S-AflII (5 ng in 50 µl reaction) using primers introducing poly-A linkers and sequences corresponding to H101 of 23S rRNA (underlined) and h44 in 16S rRNA (italicized) TTAGTACCGGTTAGCTCAACGCATCG(T)$_{7\text{-}12}$*CGAAGGTTAAGCTACCTACTTCTTTTGC* (reverse primer with tether T1) and TTG

ATAGGCCGGGTGTGTAAGCGCAG$(A)_{7\text{-}12}$*GGAGGGCGCTTACCACTTTGT* (forward primer with tether T2). The PCR reaction, which was catalysed by Phusion High Fidelity DNA polymerase, was carried out under the following conditions: 98 °C for 2 min followed by 30 cycles of (98 °C, 30 s; 62 °C, 30 s; 72 °C, 2 min) followed by 72 °C for 5 min. The resulting 4.6-kilobase (kb) PCR fragment was treated with DpnI for 4 h at 37 °C and purified using Wizard SV Gel and PCR Clean-Up kit (Promega). The PCR-amplified plasmid backbone and the gel-purified CP2861 23S rRNA gene fragment were combined in a Gibson Assembly reaction. Five microlitres of the reaction mixture was transformed into 50 µl electrocompetent POP2136 *E. coli* cells. Cells were plated onto LB/agar plate supplemented with 100 µg ml^{-1} ampicillin. After 24 h incubation at 30 °C, the colonies appeared. Seventeen colonies were picked, grown in LB/ampicillin at 30 °C, plasmids were isolated and linkers were sequenced using the primers 5′-GAACCTTACCTGGTCTTGACATC-3′ (corresponding to the 16S rRNA sequence 976–998) and 5′-ATATCGACGGCGGTGTTTG-3′ (corresponding to the 23S rRNA sequence 2476–2495) to verify the complexity of the linker library (Supplementary Table 2). All the colonies were then washed off the plate and total plasmid was extracted and used to transform SQ171-competent cells.

Functional replacement of the wild-type ribosome by Ribo-T. SQ171 cells carrying the pCSacB plasmid, which contains the wild-type *rrnB* operon, were transformed with the total pRibo-T preparation isolated from the POP2136 cells. In brief, 250 ng of plasmid preparation were added to 250 µl of rubidium-chloride-competent cells. Cells were incubated for 45 min on ice, 45 s at 42 °C and then 2 min on ice followed by addition of 1 ml SOC medium and incubation at 37 °C for 2 h with shaking. A 150-µl aliquot of the culture was transferred to 1.85 ml SOC supplemented with 100 µg ml^{-1} ampicillin and 0.25% sucrose (final concentrations) and grown overnight at 37 °C with shaking. Cells were spun down and plated on an LB agar plate containing 100 µg ml^{-1} ampicillin, 5% sucrose and 1 mg ml^{-1} erythromycin. Eighty of the colonies that appeared after 48-h incubation of the plate at 37 °C were inoculated in 2 ml LB supplemented with 100 µg ml^{-1} ampicillin and grown for 48 h. The growth rate of ~30 clones that managed to grow during that period was then assessed in LB/ampicillin medium in the 96-well plate. Plasmids were isolated from six faster growing clones and linkers were sequenced. The linker T1 in five sequenced clones was composed of 9 adenines and linker T2 was composed of 8 adenines, while one clone had the reverse combination. Total RNA was extracted from these clones using RNeasy Mini Kit (Qiagen) and analysed by agarose electrophoresis. The successful replacement of the wild type pCSacB plasmid with the pRibo-T plasmids carrying Ribo-T was verified by PCR using primers 5′-GACAGTTCGGTCCCTATCTG-3′ (corresponding to the 23S rRNA sequence 2599–2618) and 5′-TTAAGCCTCACG GTTCATTAG-3′ (complementary to the 23S rRNA sequence 2880–2900) and additionally verified by primer extension on the total cellular rRNA as indicated in the Extended Data Fig. 4. The growth of the cells was monitored at 37 °C in 150 µl of LB supplemented with 100 µg ml^{-1} of ampicillin in the wells of a 96-well plate in the TECAN microplate reader (15 min orbital shaking with a 3-mm amplitude followed by 5 min rest before reading). The doubling time (τ) values estimated from the logarithmic parts of the growth curves are indicated in Extended Data Fig. 4a.

Polysome analysis. The cultures of cells (250 ml) of the SQ171fg strain transformed with either pAM552 (wild-type) or pRibo-T8/9 were grown at 37 °C with vigorous shaking. When the optical density reached $A_{600\ nm}$ 0.4–0.7, chloramphenicol solution was added to obtain final concentration of 125 µg ml^{-1} and, after 5 min, cells were pelleted by centrifugation at 4 °C. Polysomes were prepared following the published protocol[29] by freeze-thawing in the lysis buffer (20 mM Tris-HCl, pH 7.5, 15 mM $MgCl_2$) supplemented with 1 mg ml^{-1} lysozyme 0.25% sodium deoxycholate and 2 U of RQ1 DNase (Promega). The lysates were centrifuged at 20,000*g* for 30 min at 4 °C and polysomes-containing supernatants (20 $A_{260\ nm}$ absorbance units) were loaded onto the 12-ml 10–50% sucrose gradient (buffer: 20 mM Tris-HCl, pH 7.5, 10 mM $MgCl_2$, 100 mM NH_4Cl_2, 2 mM β-mercaptoethanol). Polysomes were resolved by centrifugation in a SW-41 rotor (39,000 r.p.m., 3 h, 4 °C). Gradients were fractionated using BioComp Instrument gradient fractionator and fractions were collected in the wells of a 96-well plate. Appropriate fractions were pooled, ribosomes were ethanol-precipitated and resuspended in 200 µl of buffer containing 300 mM sodium acetate, pH 5.5, 5 mM EDTA, 0.5% SDS. rRNA was isolated by successive extractions with phenol (pH 6.6), phenol/chloroform and chloroform. After ethanol precipitation, RNA was analysed by non-denaturing agarose gel electrophoresis.

Analysis of protein synthesis rate and proteins synthesized in Ribo-T cells. The protein synthesis rate in SQ171fg cells expressing either wild-type ribosomes (plasmid pAM552) or Ribo-T (pRibo-T plasmid) was measured by following incorporation of [^{35}S]L-methionine into proteins as described[30]. Specifically, 0.25 µCi of [^{35}S]L-methionine (specific activity 1,175 Ci mmol^{-1}) (American Radiolabeled Chemicals) was added to 1 ml of exponentially growing cells at 37 °C, and after a 45 s incubation, proteins were precipitated by addition of 1 ml of ice-cold 25% trichloroacetic acid (TCA) containing 2% casamino acids. After incubating for 30 min on ice and then 30 min at 100 °C, samples were passed through G4 glass fibre filters. The filters were washed three times with 3 ml of ice-cold 5% TCA, and once with 3 ml of acetone and air dried, and the amount of retained radioactivity was determined by scintillation counting. Preliminary measurements of the time course of [^{35}S]L-methionine incorporation in the faster-growing SQ171fg/pAM552 cells showed that radioactivity curve plateaus after 120 s of incubation of cells with [^{35}S]L-methionine.

Exponential cultures (250 ml) of the SQ171fg strain transformed with either pAM552 (A2058G) or pRibo-T8/9 growing in LB medium supplemented with 100 µg ml^{-1} ampicillin and 50 µg ml^{-1} spectinomycin were collected by centrifugation and cells were flash-frozen in liquid nitrogen. Protein isolation and two-dimensional gel electrophoresis was performed by Kendrick Labs.

Preparation of Ribo-T and wild-type ribosomes and analysis of their RNA and protein content. Ribosomes were prepared from the exponentially growing cells of the SQ171fg strain transformed with either pAM552 (wild-type) or pRibo-T8/9 as described[31]. RNA was phenol extracted, precipitated as previously described and resolved by electrophoresis in a denaturing 6% (acrylamide:bis-acrylamide ratio 1:19, w/w) polyacrylamide gel (for the 5S rRNA analysis) or 4% (acrylamide:bis-acrylamide ratio 1:29, w/w) polyacrylamide gel (for the analysis of large rRNAs).

Ribo-T-associated ribosomal proteins were analysed by mass spectrometry at the Proteomics Center of Excellence, Northwestern University. Ribosomes were precipitated by incubation in 20% trichloracetic acid at 4 °C overnight and centrifugation at 14,000*g* for 10 min. Precipitated ribosomes were washed once with cold 10% trichloracetic acid and twice with acetone. The pellet was air-dried for 10–20 min before resuspension in 20 µl 8 M urea. Proteins were reduced with 10 mM dithiothreitol, and cysteine residues alkylated with 50 mM iodoacetamide in the final volume of 160 µl. Sequencing-grade trypsin (Promega) was added at a 1:50 enzyme:protein ratio, and after overnight digestion at room temperature, the reaction was stopped by addition of formic acid to 1%. After digestion, peptides were desalted using C18 Spin columns (Pierce, 89870) and lyophilized. Amino-reactive tandem mass tag (TMT) reagents (126/127, Thermo Scientific, 90065) were used for peptide labelling. The reagents were dissolved in 41 µl acetonitrile and added to the lyophilized peptides dissolved in 100 µl of 100 mM triethylammonium bicarbonate. After 1 h at room temperature, the reaction was quenched by adding 8 µl of 5% hydroxylamine. After labelling, the two samples under analysis were mixed in 1:1 ratio. Peptides were desalted using C18 ZipTip Pipette Tips (EMD Millipore) and resuspended in 30 µl of solvent A (95% water, 5% acetonitrile, 0.2% formic acid).

Peptides were analysed using nanoelectrospray ionization on an Orbitrap Elite mass spectrometer (Thermo Scientific). Proteome Discoverer (Thermo Scientific) and the Sequest algorithm were used for data analysis. Data were searched against a custom database containing UniProt entries using *E. coli* taxonomy, allowing three missed cleavages, 10 p.p.m. precursor tolerance, and carbamidomethylation of cysteine as a static modification. Variable modifications included oxidation of methionine, TMT of lysine and amino-terminal TMT. For quantification via the reporter ions the intensity of the signal closest to the theoretical *m/z*, within a ±10-p.p.m. window, was recorded. Reporter ion intensities were adjusted based on the overlap of isotopic envelopes of all reporter ions as recommended by the manufacturer. Only peptides with high confidence were used for quantification. Ratios of 126/127 were normalized based on median.

Sucrose gradient analysis of ribosomes and ribosomal subunits. Wild-type 70S ribosomes or Ribo-T isolated from SQ171fg cells as described above were diluted approximately 70-fold in high Mg^{2+} buffer (20 mM Tris-HCl, pH 7.5, 100 mM NH_4Cl, 2 mM 2-mercaptoethanol, 15 mM $MgCl_2$) or low Mg^{2+} buffer (20 mM Tris-HCl, pH 7.5, 100 mM NH_4Cl, 2 mM 2-mercaptoethanol, 1.5 mM $MgCl_2$). After incubation for 30 min at 4 °C, ribosomes and subunits were resolved in 10–40% 12-ml sucrose gradients prepared with the same buffers. Gradients were centrifuged in the SW41 rotor at 38,000 r.p.m. for 3 h at 4 °C. Ribosome profiles were then analysed using gradient fractionator (BioComp Instrument).

Probing the structure of the Ribo-T tethers. The structure of the tethers was probed by dimethylsulfate (DMS) modification following a published protocol[32]. In brief, 10 pmol of Ribo-T or wild-type ribosomes were activated by incubation for 5 min at 42 °C in 50 µl of buffer 80 mM HEPES-KOH, pH 7.6, 15 mM $MgCl_2$, 100 mM NH_4Cl containing 20 U of RiboLock RI RNase inhibitor (Thermo Fisher Scientific). Two microlitres of DMS (SIGMA) diluted 1:10 in ethanol were added (2 µl of ethanol were added to the unmodified controls) and samples were incubated for 10 min at 37 °C. The modification reaction was stopped and rRNA extracted as described[32]. Primer extensions were carried out using the primers 5′-GACTGCCAGGGCATCCACCG-3′ and 5′-AAGGTTAAGCCTCACGG-3′ (for tether T1) or 5′-CCCTACGGTTACCTTGTTACG-3′ for tether T2.

Additionally, the integrity of the tethers in the Ribo-T preparation was tested by extension of the primers annealing immediately 3′ to the tether. Primer 5′-GTACCGGTTAGCTCAACGCATC-3′ was extended by reverse transcriptase across tether T1 in the presence of dATP, dTTP, dGTP and ddCTP, and primer 5′-CACAAAGTGGTAAGCGCCCTCCT-3′ was extended across tether T2 in the presence of dATP, dTTP, dCTP and ddGTP.

Testing Ribo-T activity in cell-free translation system. The DNA template containing the T7 promoter and the sf-GFP gene[14] was PCR amplified from a pY71-sfGFP plasmid[33] using primers 5′-TAATACGACTCACTATAGGG-3′ and 5′-CTTCCTTTCGGGCTTTGTT-3′. GFP mRNA was prepared by *in vitro* transcription and purified by size-exclusion chromatography on a Sephadex G50 mini-column, phenol extraction and ethanol precipitation. The transcript was translated in the Δ(ribosome, amino acid, tRNA) PURExpress system kit (New England Biolabs). A typical translation reaction was assembled in a total volume of 10 μl and contained 2 μl of the kit solution A, 1.2 μl of factor mixture, 1 μl amino acid mixture (3 mM each), 1 μl tRNA (20 μg ml^{-1}), 0.4 μl Ribolock RNase inhibitor (40 U μl^{-1}), 5 μg (~20 pmol) GFP transcript and 22 pmol of wild-type ribosomes or Ribo-T. Samples were placed in wells of a 384-well black wall/clear flat bottom tissue-culture plate (BD Biosciences) and covered with the lid. Reactions were incubated at 37 °C in a microplate reader (Tecan), and fluorescence values were recorded every 20 min at $\lambda_{exc} = 488$ nm and $\lambda_{em} = 520$ nm over 7 h. Protein synthesis rates were calculated by linear regression over the time points 0, 40 and 60 min with a $R^2 > 0.9$ using the trendline function of Excel (Microsoft). Time point 20 min was not taken into consideration because the plate was switched from ice to 37 °C at time 0.

Transcription/translation of the dihydrofolate reductase template supplied with the Δ(ribosome, amino acid, tRNA) PURExpress kit (New England Biolabs) was carried in the presence of [^{35}S]L-methionine (1,175 Ci mmol^{-1}) using manufacturers protocol. A typical 5 μl reaction, assembled as described above but using 50ng of the DNA template, was supplemented with 5 μCi [^{35}S]L-methionine and 10 pmol of wild-type or Ribo-T ribosomes. When needed, the reactions were supplemented with 50 μM erythromycin. Reactions were incubated for 2 h at 37 °C, and protein products were analysed by SDS–PAGE in 16.5% Bis-Tris gels (Biorad) using NuPAGE MES/SDS running buffer (Invitrogen). Gels were stained, dried and exposed to a phosphorimager screen overnight. Radioactive bands were visualized by Typhoon phosphorimager (GE Healthcare).

Toeprinting analysis. Toeprinting was performed as previously described[15,34]. When needed, the threonyl-tRNA synthetase inhibitor borrelidin or the initiation inhibitor thiostrepton were added to the reactions to the final concentrations of 50 μM.

Construction of the plasmids for testing oRibo-T activity *in vivo*. The backbone plasmid pT7wtK (Extended Data Fig. 1c) was first prepared from the commercial plasmid T7-Flag-4 (Sigma Aldrich) by introducing the following changes. First, the *bla* gene was deleted using inverse PCR with phosphorylated primers 5′-TAACTGTCAGACCAAGTTTACTC-3′ and 5′-ACTCTTCCTTTTTCAATATTATTGAAG-3′ and Phusion High Fidelity DNA polymerase. Following purification with E.Z.N.A. Cycle Pure kit, DNA was blunt-end ligated for 14 h at 16 °C using T4 DNA ligase, and transformed into electrocompetent DH5α *E. coli* cells and plated on LB-agar supplemented with 30 μg ml^{-1} kanamycin. Next, a BglII-NotI cloning site was introduced using phosphorylated primers 5′-**AGATCT**GTTGCTACGCAGCGTT**GCGGCCGC**TGAAGATCGATCTCGACG-3′ and 5′-GCCTCCTATGAAAAAATAACAGATATAGTCTCCCTATAGTGAGTCGTATTAGG-3′, with BglII and NotI sites in bold. A sequence 3′ of the T7 promoter, termed N15 (underlined), optimized for T7 expression of an orthogonal gene[35] was introduced on one of the primers. Purified PCR product was blunt-end ligated with T4 DNA ligase for 14 h at 16 °C, transformed into DH5α electrocompetent cells and plated on LB-agar supplemented with 30 μg ml^{-1} kanamycin. The resulting plasmid pT7wtK contains a T7 promoter, wild-type Shine–Dalgarno sequence, a BglII-NotI cloning site, T1/T2 terminator, pMB1 origin of replication, a *lacI* gene and a kanamycin resistance gene.

To create plasmid pT7wtGFP, primers 5′-GGTGGT**AGATCT**ATGAGCAAAGGTGAAGAAC-3′ and 5′-GGTGGT**GCGGCCGC**GGGCTTTGTTAGCAG-3′ were used to PCR amplify the *sf-gfp* gene from pY71-sfGFP[33], adding BglII and NotI restriction sites (bold) at the ends of the *sf-gfp* PCR product. Purified PCR product and plasmid pT7wtK were digested with BglII and NotI (New England Biolabs) for 1 h at 37 °C. The pT7wtK digested vector was treated with alkaline phosphatase CIP (New England Biolabs) for 1 h at 37 °C. Both reactions were purified with E.Z.N.A. Cycle Pure kit. The *sf-gfp* insert was added in threefold molar excess to 50 ng pT7wtK backbone, and ligated with T4 DNA ligase (NEB) for 14 h at 16 °C, transformed into DH5α electrocompetent cells and plated on LB-agar supplemented with 30 μg ml^{-1} kanamycin.

To create pT7oGFP (Extended Data Fig. 1c) containing *sf-gfp*, the translation of which is controlled by an orthogonal Shine–Dalgarno sequence, the wild-type Shine–Dalgarno sequence of pT7wtGFP (AGGAGG) was mutated to an orthogonal sequence CACCAC (ref. 3) by inverse PCR using phosphorylated primers 5′-ATGAGCAAAGGTGAAGAAC-3′ and 5′-AGATCTGTGGTGTGAAAAAATAACAGATATAGTCTC-3′. PCR product purified with E.Z.N.A. Cycle Pure kit was blunt-end ligated with T4 DNA ligase for 14 h at 16 °C, transformed into electrocompetent DH5α cells and plated on LB-agar supplemented with 30 μg ml^{-1} kanamycin.

Finally, the T7 promoter was replaced with the lpp5 promoter[36]. To achieve that, inverse PCR was performed using pT7oGFP as template and phosphorylated primers 5′-TATACTTGT**GGAATTGTGAGCGGATAACAATT**CTATATCTGTTATTTTTTCA-3′ and 5′-ACACAAAGTTTTTTATGTTGTCAATATTTTTTTGATAGTGAGTCGTATTAGGATC-3′, (the lpp promoter is underlined). The *lacO* site (bold) was included to provide for inducible expression in POP2136 strain controlled with IPTG. DNA was purified, blunt-end ligated, transformed into DH5α cells and plated on LB-agar supplemented with 30 μg ml^{-1} kanamycin. The resulting plasmid pLpp5oGFP (Extended Data Fig. 1c) contains a lpp5 promoter, *lac*O site, orthogonal Shine–Dalgarno sequence, *sf-gfp* gene, T1/T2 terminator, pMB1 origin of replication, a *lacI* gene and a kanamycin-resistance gene.

The anti-Shine–Dalgarno sequence of pRibo-T 16S rRNA was mutated from wild-type (5′-TCA**CCTCCT**TA-3′) to an orthogonal sequence (5′-TCA**TTGTGG**TA-3′)[3] by inverse PCR using phosphorylated primers 5′-CCTTAAAGAAGCGTACTTTGTAG-3′ and 5′-TACCACAATGATCCAACCGCAGG-3′, pRibo-T as template and Phusion High Fidelity DNA polymerase. PCR was run at the following conditions: 98 °C, 3 min followed by 25 cycles (98 °C, 30 s; 55 °C, 30 s; 72 °C, 120 s), followed by final extension 72 °C, 10 min. Correct size band was purified by agarose gel electrophoresis and extracted using the E.Z.N.A. Gel Extraction kit. It was circularized by blunt-end ligation and transformed into POP2136 electrocompetent cells. Cells were plated on LB/agar plates supplemented with 50 μg ml^{-1} carbenicillin and grown at 30 °C overnight. Colonies were isolated and poRibo-T was fully sequenced.

Testing activity of oRibo-T *in vivo*. Electrocompetent POP2136 cells were transformed with the following plasmid combinations: (1) pAM552 and pT7wtK (no *gfp* control), (2) pAM552 and pLpp5oGFP, (3) pAM552o and pLpp5oGFP, and (4) poRibo-T1 and pLpp5oGFP. Transformants were plated on LB plates supplemented with 50 μg ml^{-1} carbenicillin and 30 μg ml^{-1} kanamycin and incubated for 24 h at 30 °C. Wells of a 96-well plate with low evaporation lid (Costar) was filled with 100 μl of LB media supplemented with 50 μg ml^{-1} carbenicillin and 30 μg ml^{-1} kanamycin. The wells were inoculated with colonies from each plasmid combination above (six colonies each), and incubated at 30 °C for 14 h with shaking. Clear bottom chimney wells of another 96-well plate (Costar) were filled with 100 μl of LB media supplemented with 50 μg ml^{-1} carbenicillin, 30 μg ml^{-1} kanamycin, and 1 mM IPTG. The plate was inoculated with 2 μl of saturated initial inoculation plate, and incubated with linear shaking (731 cycles per min) for 16 h at 42 °C on a Biotek Synergy H1 plate reader, with continuous monitoring of cell density ($A_{600\ nm}$) and sfGFP fluorescence (excitation 485 and emission 528 with sensitivity setting at 80).

Testing oRibo-T activity in cell-free translation system. Ribosomes (wild-type) or oRibo-T (mixed with wild-type ribosomes) were prepared from SQ171fg cells transformed with pAM552 or poRibo-T1, respectively. An orthogonal *sf-gfp* gene was PCR amplified from the plasmid pT7oGFP using primers 5′-TAATACGACTCACTATAGGG-3′ and 5′-ACTCGTCGAGATCGATCT-3′. The transcription-translation reaction was carried out in Δ(ribosome, amino acid, tRNA) PURExpress system as described above. The 7.5-μl reactions were supplemented with 18.75 ng DNA template and 7.5 pmol ribosomes, and when needed, clindamycin or pactamycin were added to the reactions to the final concentrations of 50 μM or 100 μM, respectively.

For *in vitro* translation of an orthogonal *secM-lacZa* template, it was PCR-amplified from the poSML plasmid using a direct primer 5′-TAATACGACTCACTATAGGG-3′ corresponding to the T7 promoter and a reverse primer 5′-TTCCCAGTCACGACGTT-3′, which allowed preserving 18 codons after the SecM arrest site. mRNA was prepared by *in vitro* transcription and purified. It was then translated in the Δ(ribosome, amino acid, tRNA) PURExpress system assembled in a total volume of 5 μl and containing 1 μl of the kit solution A, 0.6 μl of factor mixture, 0.5 μl amino acid mixture (3 mM each) lacking methionine, 0.2 μl of [^{35}S]L-methionine 8.5 μM (1,175 Ci mmol^{-1}), 0.5 μl tRNA (20 μg ml^{-1}), 0.2 μl Ribolock RNase inhibitor (40 U μl^{-1}), 100 μM pactamycin, 10 pmol transcript and 10 pmol of total ribosomes. Translation was carried out for 5 min at 37 °C, followed by addition of 1 μg of RNase A and incubation for 5 min at 37 °C. Translation products were analysed in 16.5% Tricine SDS–PAGE[37]. The gel was stained, dried, and exposed to a phosphorimager screen overnight.

Construction of C41(DE3)/Δ*lacZ58*(M15). The *ΔlacZ58*(M15) allele required for alpha complementation was transduced from the *E. coli* strain K1342 (*E. coli* Genetic Stock Center, Yale) into *E. coli* C41(DE3) strain by P1 phage transduction protocol[38]. Transductants were selected on LB agar supplemented with 10 μg ml^{-1}

tetracycline. Then colonies were re-streaked on LB-agar plates containing 10 μg ml^{-1} tetracycline, 200 μM IPTG and 80 μg ml^{-1} X-Gal. The replacement of wild-type *lacZ* with the *ΔlacZ58*(M15) allele was verified by PCR using primers 5′-ACCATGATTACGGATTCACTGG-3′ and 5′-CCGTTGCACCACAGATG AA-3′ (the sizes of the expected PCR products are 467 bp for wild-type and 374 bp for the mutant).

Construction of the orthogonal SecM-lacZα reporter poSML. The backbone of the pACYC177 vector was PCR-amplified using primers 5′-ATCTCATGACCAA AATCCCTTAACGTGAGT-3′ and 5′-GCGGTTAGCTTTTACCCCTGCATCT TTGAG-3′. A 568-bp DNA fragment in which the ends overlapped with the amplified pACYC177 backbone and which contained T7 promoter, the orthogonal Shine–Dalgarno sequence CACCAC[3], the *secM*(121–166)-*lacZa* fusion from the plasmid pNH122 (ref. 18), was synthesized by Integrated DNA Technologies. The pACYC177 backbone and the *secM-lacZa* construct were combined using Gibson Assembly and introduced in the C41(DE3)/ΔlacZ58(M15) cells.

Construction of the 2451/2452 mutant poRibo-T library and selecting mutants capable of alleviating SecM-mediated translation arrest. A library of A2451N/C2452N mutants was generated by inverse PCR using plasmid poRibo-T2 as a template, Phusion High Fidelity DNA polymerase, and primers 5′-AGGC TGATACCGCCCAAG-3′ and 5′-CTCTTGGGCGGTATCAGCCT**NN**TATCC CCGGAGTACCTTTTATC-3′, with added sequence (underlined) used for re-circularization with Gibson assembly. PCR reaction was carried out under the following conditions: 98 °C, 3 min followed by 25 cycles (98 °C, 30 s; 55 °C, 30 s; 72 °C, 120 s), followed by final extension 72 °C, 10 min. The PCR-amplified DNA band was purified by extraction from the agarose gel with an E.Z.N.A. gel extraction kit, and re-circularized by Gibson assembly for 1 h at 50 °C. Two microlitres of the reaction were transformed into electrocompetent POP2136 cells plated on LB plates supplemented with 50 μg ml^{-1} carbenicillin and grown for 24 h at 30 °C. Individual colonies were picked and sequenced to identify all possible 16 variants of the library.

The C41(DE3)/*ΔlacZ58*(M15) cells were transformed with the poSML reporter plasmid (Extended Data Fig. 1d) and plated on LB-agar containing 50 μg ml^{-1} kanamycin. One of the colonies, which appeared after overnight incubation at 37 °C, was inoculated into liquid culture, grown in the presence of 50 μg ml^{-1} kanamycin and cells were rendered chemically competent. Cells were transformed with the pooled library of 16 2451/2452 mutants. Transformed cells were plated on LB agar containing 50 μg ml^{-1} kanamycin, 100 μg ml^{-1} ampicillin, 0.5 mM IPTG, 40 μg ml^{-1} X-Gal and 2 mM lacZ inhibitor phenylethyl-β-d-thiogalactopyranoside (PETG). Plates were incubated at 37 °C for 24 h and photographed. Sixteen white colonies or fifteen blue colonies were inoculated in 5 ml of LB medium supplemented with 100 μg ml^{-1} ampicillin and grown overnight. The plasmids were isolated and the identities of nucleotide residues at the position 2451 and 2452 of the 23S rRNA were analysed by sequencing. Alternatively, the poSML-transformed C41(DE3)/ΔlacZ58(M15) cells were transformed with individual plasmids representing all possible 16 variants of the nucleotide combinations at positions 2451 and 2452. The poRibo-T2 plasmid carrying A2058G mutation was used as a control. In addition, the poRibo-T2 plasmid carrying the U2585G mutation was included in the transformation experiment. The transformed cells were plated on LB/agar containing 50 μg ml^{-1} kanamycin and 100 μg ml^{-1} ampicillin and incubated overnight at 37 °C. Three colonies from each transformation were then streaked on LB/agar plates containing 50 μg ml^{-1} kanamycin and 100 μg ml^{-1} ampicillin and supplemented with 0.5 mM IPTG, 40 μg ml^{-1} X-Gal and 2 mM PETG. Plates were incubated at 37 °C for 22 h and photographed.

28. Gibson, D. G. *et al.* Enzymatic assembly of DNA molecules up to several hundred kilobases. *Nature Methods* **6,** 343–345 (2009).
29. Fredrick, K., Dunny, G. M. & Noller, H. F. Tagging ribosomal protein S7 allows rapid identification of mutants defective in assembly and function of 30 S subunits. *J. Mol. Biol.* **298,** 379–394 (2000).
30. Kannan, K., Vázquez-Laslop, N. & Mankin, A. S. Selective protein synthesis by ribosomes with a drug-obstructed exit tunnel. *Cell* **151,** 508–520 (2012).
31. Ohashi, H., Shimizu, Y., Ying, B. W. & Ueda, T. Efficient protein selection based on ribosome display system with purified components. *Biochem. Biophys. Res. Commun.* **352,** 270–276 (2007).
32. Merryman, C. & Noller, H. F. in *RNA:Protein Interactions, a Practical Approach* (ed. Smith, C. W. J.) 237–253 (Oxford Univ. Press, 1998).
33. Bundy, B. C. & Swartz, J. R. Site-specific incorporation of p-propargyloxyphenylalanine in a cell-free environment for direct protein-protein click conjugation. *Bioconjug. Chem.* **21,** 255–263 (2010).
34. Vazquez-Laslop, N., Thum, C. & Mankin, A. S. Molecular mechanism of drug-dependent ribosome stalling. *Mol. Cell* **30,** 190–202 (2008).
35. An, W. & Chin, J. W. Synthesis of orthogonal transcription-translation networks. *Proc. Natl Acad. Sci. USA* **106,** 8477–8482 (2009).
36. Inouye, S. & Inouye, M. Up-promoter mutations in the *lpp* gene of *Escherichia coli*. *Nucleic Acids Res.* **13,** 3101–3110 (1985).
37. Schägger, H. & von Jagow, G. Tricine-sodium dodecyl sulfate-polyacrylamide gel electrophoresis for the separation of proteins in the range from 1 to 100 kDa. *Anal. Biochem.* **166,** 368–379 (1987).
38. Thomason, L. C., Costantino, N. & Court, D. L. E. coli genome manipulation by P1 transduction. *Curr. Prot. Mol. Biol.* **Chapter 1,** Unit–1 17 (2007).

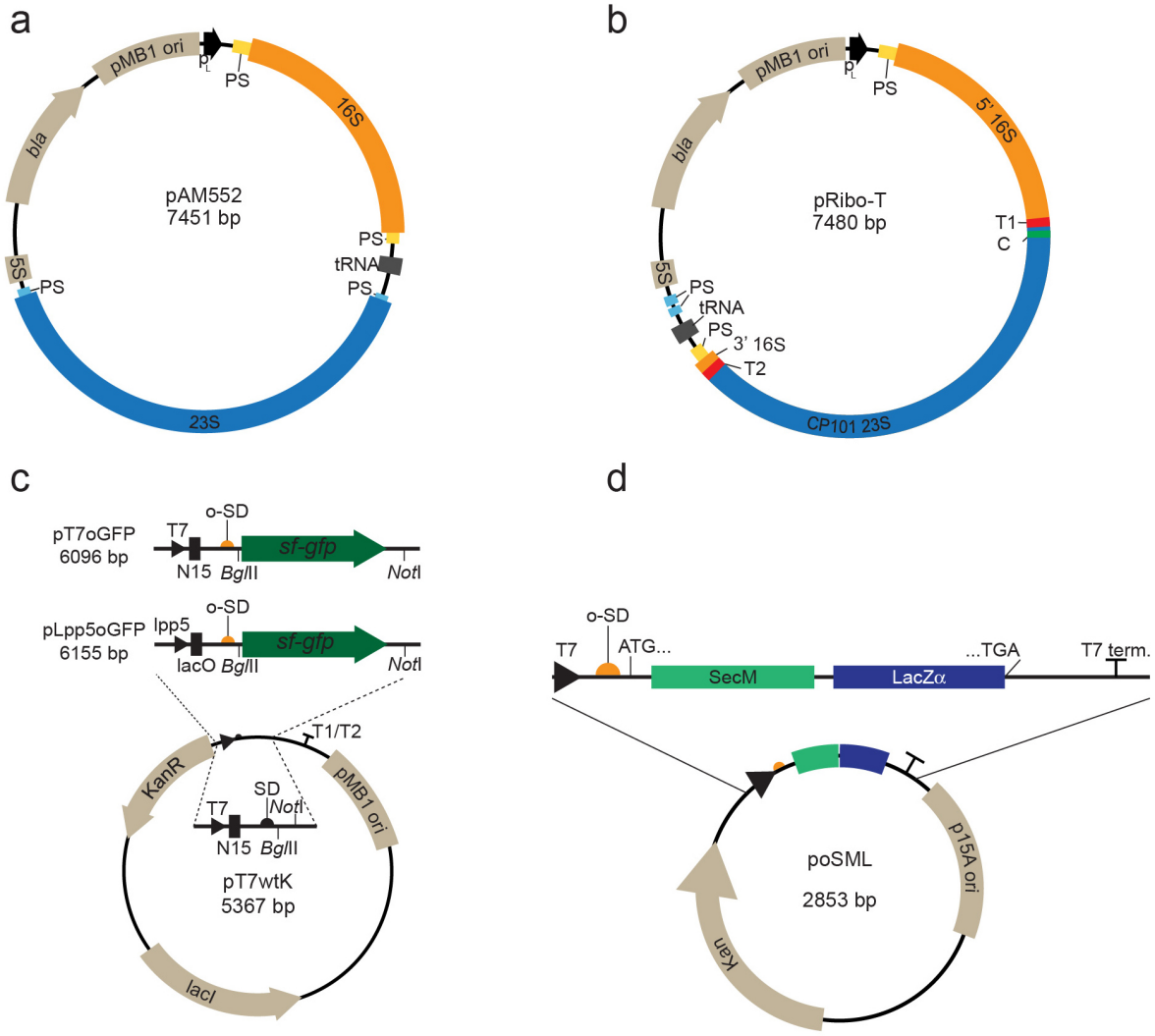

Extended Data Figure 1 | Key plasmids used in the study. **a**, The pAM552 plasmid is a derivative of pLK35 (ref. 27), from which the unessential segments of the pBR322 cloning vector have been removed. pAM552 contains the entire *rrnB* operon of *E. coli* under the control of the phage lambda P_L promoter, which is constitutively active in the conventional *E. coli* strains but is silent at 30 °C in the strain POP2136 (30 °C) carrying the *cI857* gene of the temperature-sensitive lambda repressor. The 16S rRNA gene is shown in orange, and the 16S rRNA processing stem sequences indicated in yellow. The 23S rRNA gene is blue, and the corresponding processing stem sequences are light blue. The intergenic $tRNA^{Glu}$ gene is shown in dark grey. **b**, The map of the pRibo-T8/9 plasmid derived from pAM552. The native 5′ and 3′ ends of the 23S rRNA were linked via a tetranucleotide sequence GAGA (connector C shown in green), and circularly permutated 23 rRNA gene, 'opened' in the apex loop of H101, was inserted in the apex loop of 16S rRNA helix h44 via an A_8 linker T1 and an A_9 linker T2 (red bars). **c**, The map of the backbone plasmid pT7wtK and the reporter plasmids pT7oGFP and pLpp5oGFP, expressing *sf-gfp* controlled by an orthogonal Shine–Dalgarno sequence (orange semi-circle) under T7 or lpp5 promoters (black triangles). **d**, The map of the pACYC177-derived plasmid containing the *secM-lacZa* reporter gene controlled by the T7 promoter (black triangle) and alternative Shine–Dalgarno sequence (orange semi-circle). The sequence of the *secM-lacZa* reporter matches that in the originally described plasmid pNH122 (ref. 18).

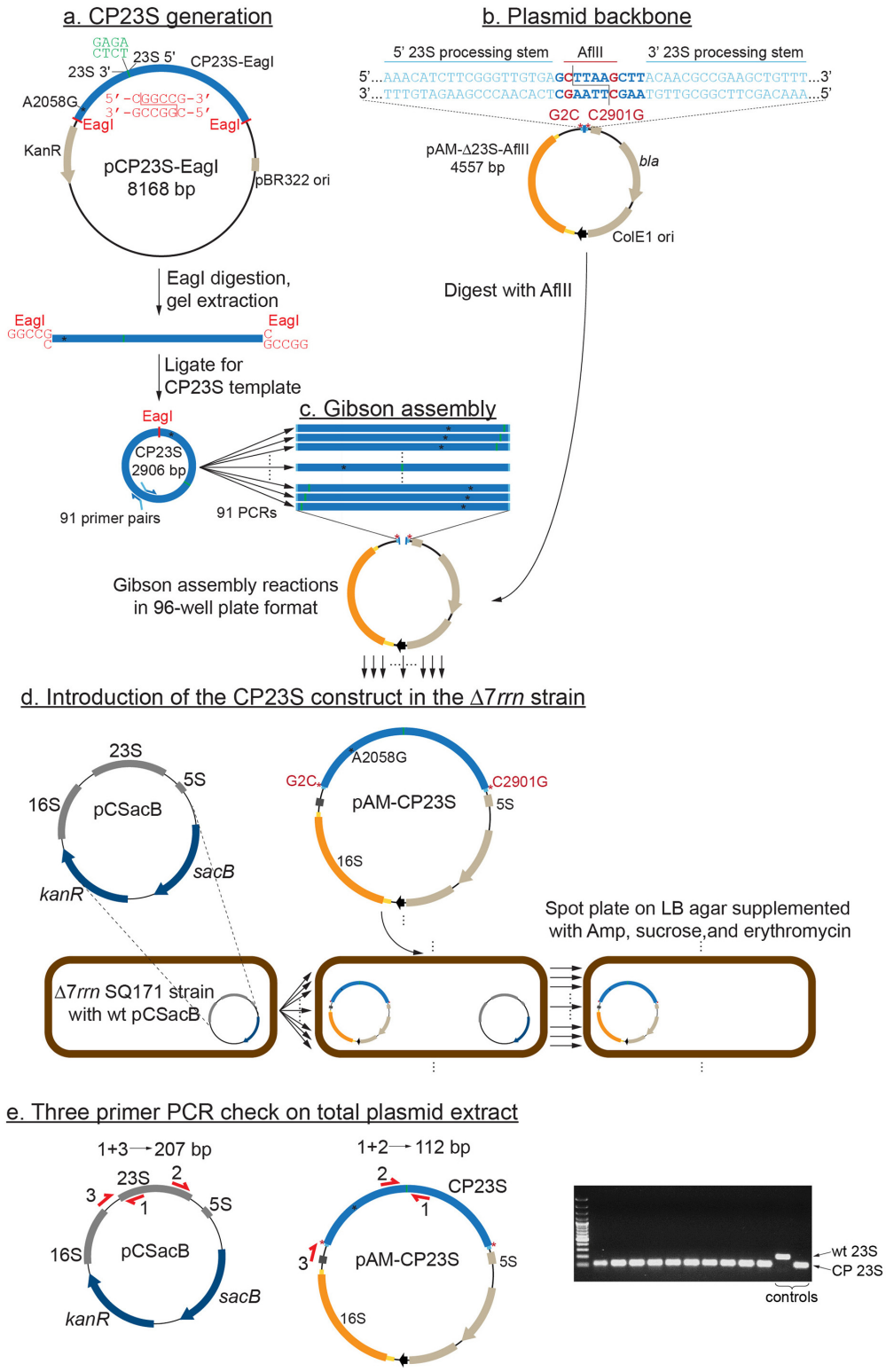

Extended Data Figure 2 | The experimental scheme of preparing and testing circularly permuted 23S rRNA gene library. **a**, The CP23S template is generated from pCP23S-EagI plasmid by EagI digestion and ligation. Each CP23S variant is generated by PCR using circularized 23S rRNA gene as a template and a unique primer pair, with added sequences overlapping the destination plasmid backbone. **b**, The plasmid backbone is prepared by digestion of pAM552-Δ23S-AflII with the AflII restriction enzyme, which linearizes the backbone at the 23S processing stem site. **c**, Gibson assembly is used to incorporate each CP23S variant into the plasmid backbone to generate the 91 target circular permutants. **d**, The pAM-CP23S plasmids are transformed into the SQ171 strain lacking chromosomal rRNA operons and carrying the pCSacB plasmid with the wild-type rRNA operon, and transformants resistant to ampicillin, erythromycin and sucrose are selected. **e**, A complete replacement of pCSacB with pAM-CP23S is verified by a three-primer diagnostic PCR.

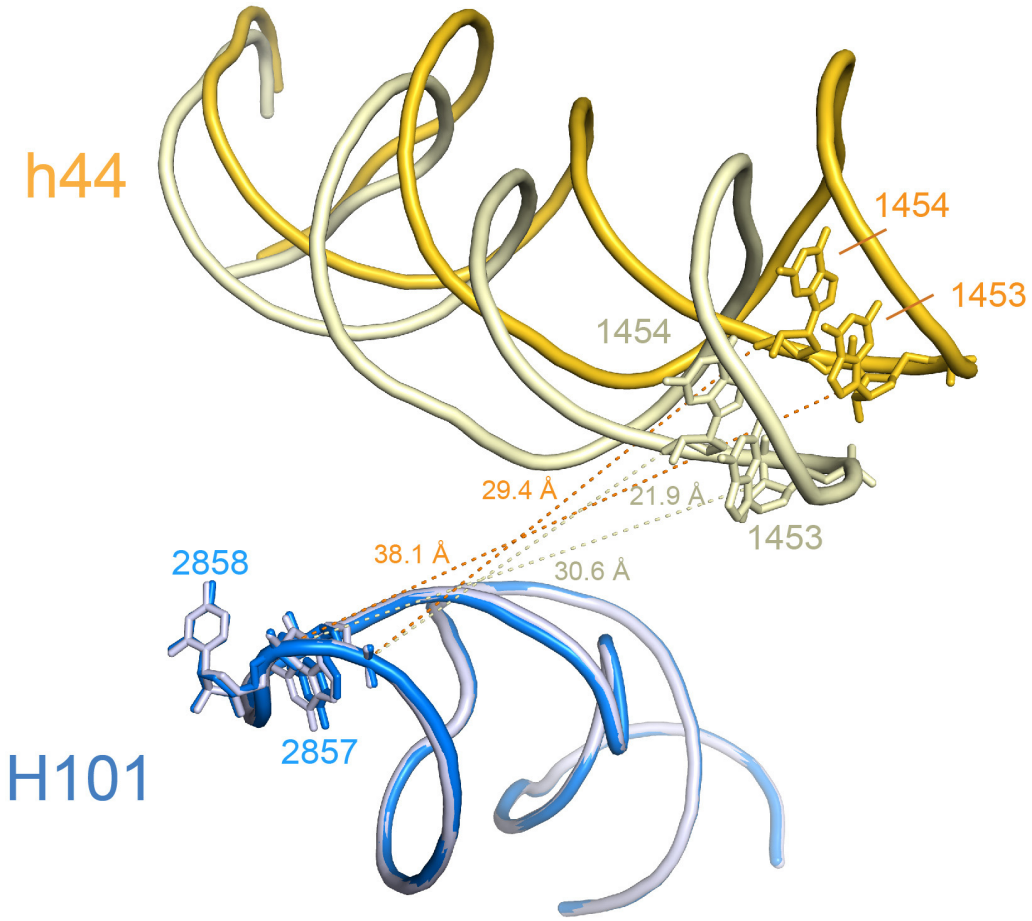

Extended Data Figure 3 | The Ribo-T tethers allow for the ribosome ratcheting. Distance changes (Å) between the 16S rRNA and 23S rRNA residues h44 and H101 connected by the oligo(A) linkers in Ribo-T when the ribosome undergoes the transition from the classic to the rotated state. The distances between the 5′ phosphorus atoms of the corresponding nucleotides are shown. 16S and 23S rRNAs in the non-rotated state are tan and pale blue, and in the rotated state are gold and blue, respectively. The structures of the *E. coli* ribosomes used for measuring the distances and generating the figure have PDB accession numbers 3R8T and 4GD2 (non-rotated state) and 3R8S and 4GD1 (rotated state).

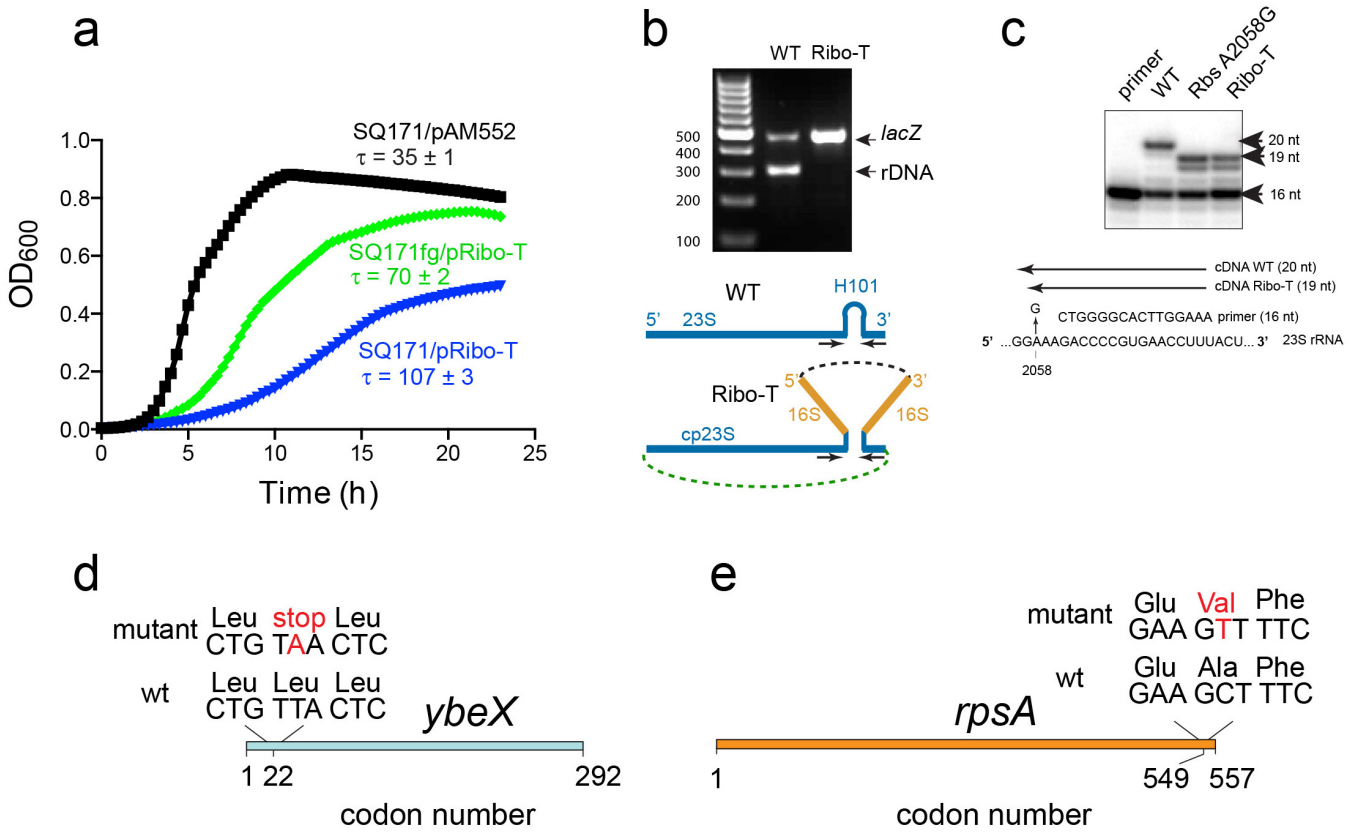

Extended Data Figure 4 | Chromosomal mutations enhance growth of SQ171 cells in which Ribo-T completely replace wild-type ribosomes. **a**, Growth curves of the parental SQ171 cells transformed with the pAM552(G2058) plasmid (black curve) or pRibo-T8/9 plasmid (blue curve) or selected fast growing mutant (SQ171fg) transformed with pRibo-T8/9 (green curve). The cells express homogeneous populations of ribosomes (wt for pAM552 transformants or Ribo-T for the pRibo-T8/9 transformants, see panels b and c). **b**, PCR analysis of rDNA in the SQ171fg strain transformed with pRibo-T8/9 (the SQ110 strain that carries a single chromosomal copy of the *rrn* allele served as a wild-type control). The PCR primers amplify the 302-base-pair 23S rRNA gene segment 'across' the H101 hairpin in wild-type rDNA. In pRibo-T, the primer annealing sites are more than 4.8 kb apart (black dashed line), which prevents formation of the PCR product. Two additional primers designed to amplify a 467-bp fragment from the *lacZ* gene were included in the same PCR reaction as an internal control. The gel is representative of two independent biological experiments. **c**, Primer extension analysis of rRNA expressed in the SQ171fg cells transformed with pAM552 (WT), pAM552 with the A2058G mutation, or pRibo-T8/9, which carries the A2058G mutation. Primer extension was carried out in the presence of dTTP and ddCTP. Because Ribo-T contains the A2058G mutation in the 23S rRNA sequence, the generated cDNA is one nucleotide shorter than the one generated on the wild-type 23S rRNA template. The lack of the 20-nucleotide cDNA band in the Ribo-T sample demonstrates the absence of wild-type 23S rRNA in the SQ171fg cells transformed with pRibo-T8/9. The gel is representative of three independent biological experiments. **d**, **e**, Chromosomal mutations in SQ171fg: a nonsense mutation in the Leu codon 22 of the *ybeX* gene encoding a protein similar to Mg^{2+}/Co^{2+} efflux transporter (**d**); and a missense mutation in codon 549 of the *rpsA* gene encoding ribosomal protein S1 (**e**).

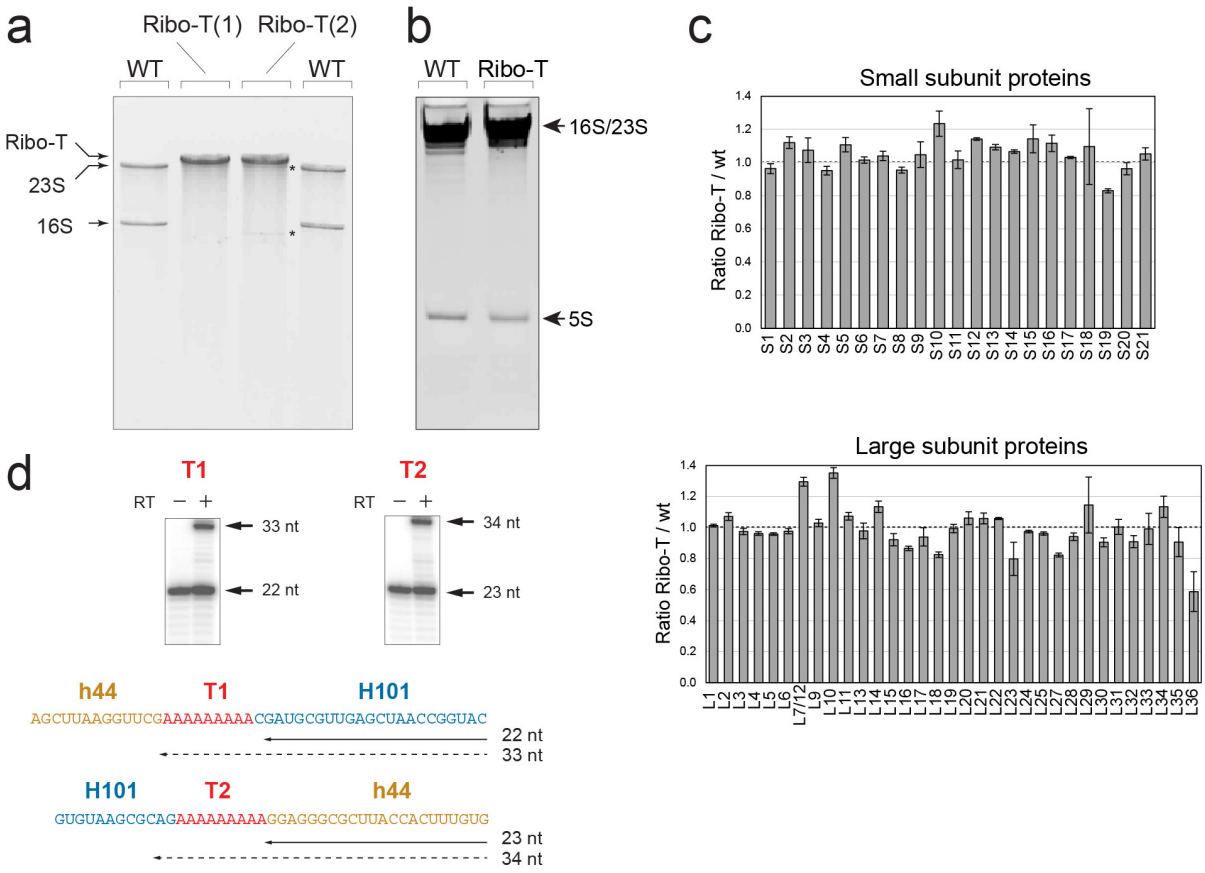

Extended Data Figure 5 | Ribo-T composition and integrity of the linkers. **a**, **b**, Analysis of rRNA extracted from the isolated wild-type ribosomes or Ribo-T in a denaturing 4% (**a**) or 8% (**b**) polyacrylamide gel. **a**, Ribo-T(1) and Ribo-T(2) represent two individual preparations with Ribo-T(2) isolated following the standard procedure (see Methods), and Ribo-T(1) isolated by immediate pelleting through the sucrose cushion after the cell lysis. The faint bands in the Ribo-T2 preparation indicated by the asterisks could be occasionally seen in some preparations; they probably represent rRNA fragments generated by cleavage of the linkers in a small fraction of Ribo-T either in the cell or during Ribo-T preparation. **b**, 5S rRNA is present in Ribo-T. **c**, The relative abundance of small and large subunit proteins in Ribo-T in comparison with wild-type ribosome as determined by mass spectrometry (protein L26 could not be reliably quantified in Ribo-T and wild-type ribosomes). The data represent the average of three technical replicates, and error bars indicate the s.d. **d**, Analysis of the integrity of the T1 and T2 linkers in a Ribo-T preparation by primer extension. The 22-nucleotide-long primer was extended across the T1 linker in the presence of ddCTP terminator and the 23S-nucleotide-long primer was extended across the T2 linker in the presence of ddGTP terminator. Control samples (−) represent the unextended primers. The gels are representative of two independent experiments.

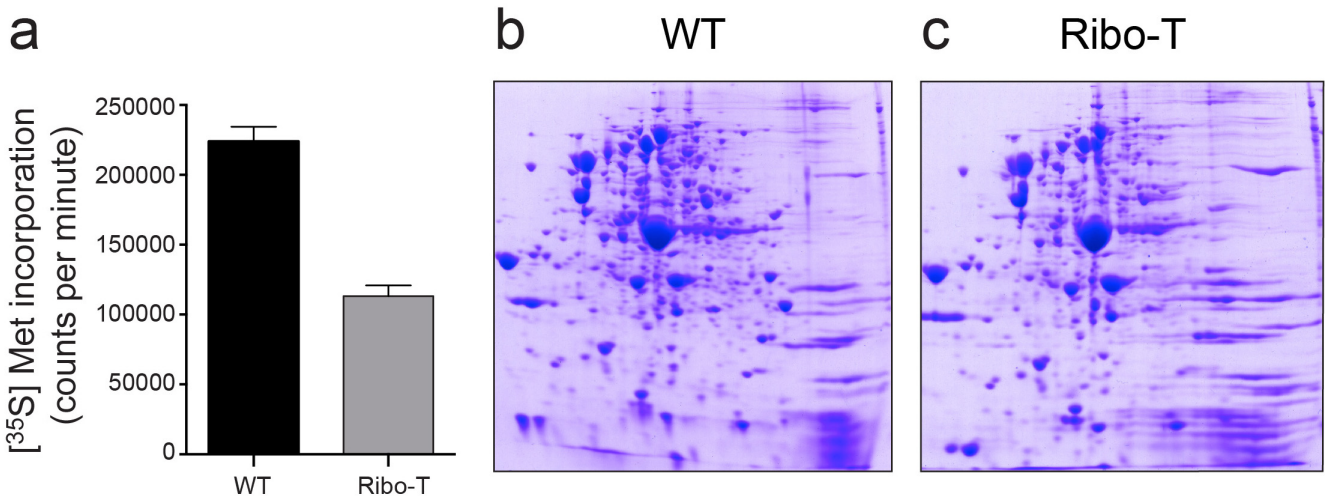

Extended Data Figure 6 | Ribo-T can successfully translate most cellular polypeptides. **a**, Protein synthesis rate in SQ171fg cells expressing wild-type ribosomes or Ribo-T. Protein synthesis was measured by quantifying the incorporation of [^{35}S] L-methionine into TCA-insoluble protein fraction during a 45-s incubation at 37 °C in minimal medium. The bar graphs represent the average values of experiments performed in two biological replicates each done in two technical duplicates. Error bars denote s.d. **b**, **c**, 2D gel electrophoresis analysis of the proteins expressed in exponentially growing SQ171fg transformed with pAM552 (A2058G) (**b**) or pRibo-T (**c**).

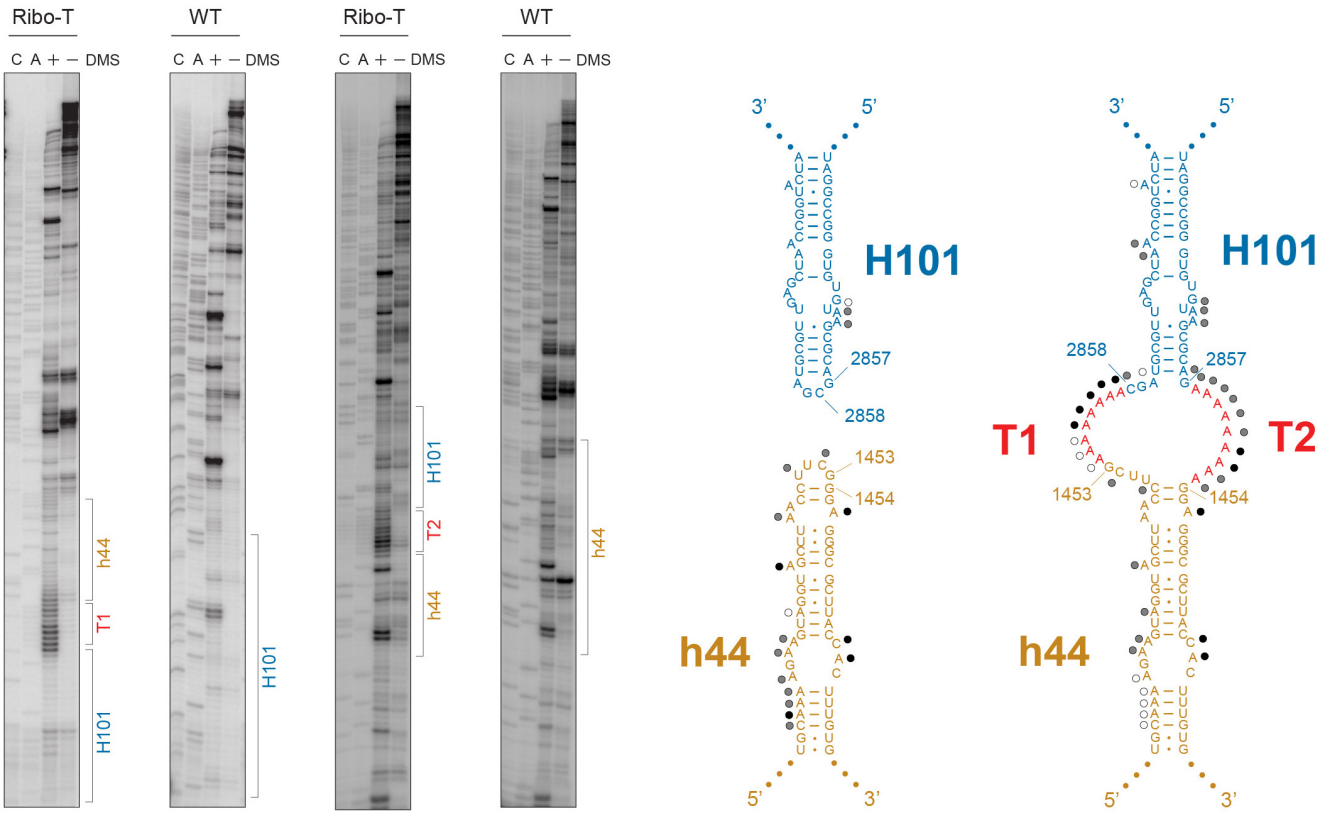

Extended Data Figure 7 | Chemical probing of the structure of the Ribo-T linkers. Ribo-T or wild-type ribosomes were modified by dimethylsulfate, and extracted rRNA was subjected to primer extension analysis. In each gel, the left two lanes ('C' and 'A') represent sequencing reactions followed by dimethylsulfate-modified sample and control (unmodified) RNA. The diagrams on the right represent the secondary structures of helices H101 and h44 in wild-type ribosomes (left) and Ribo-T (right), with the nucleotide residues modified strongly, moderately and weakly indicated by black, grey and white circles, respectively. The gels are representative of two independent experiments.

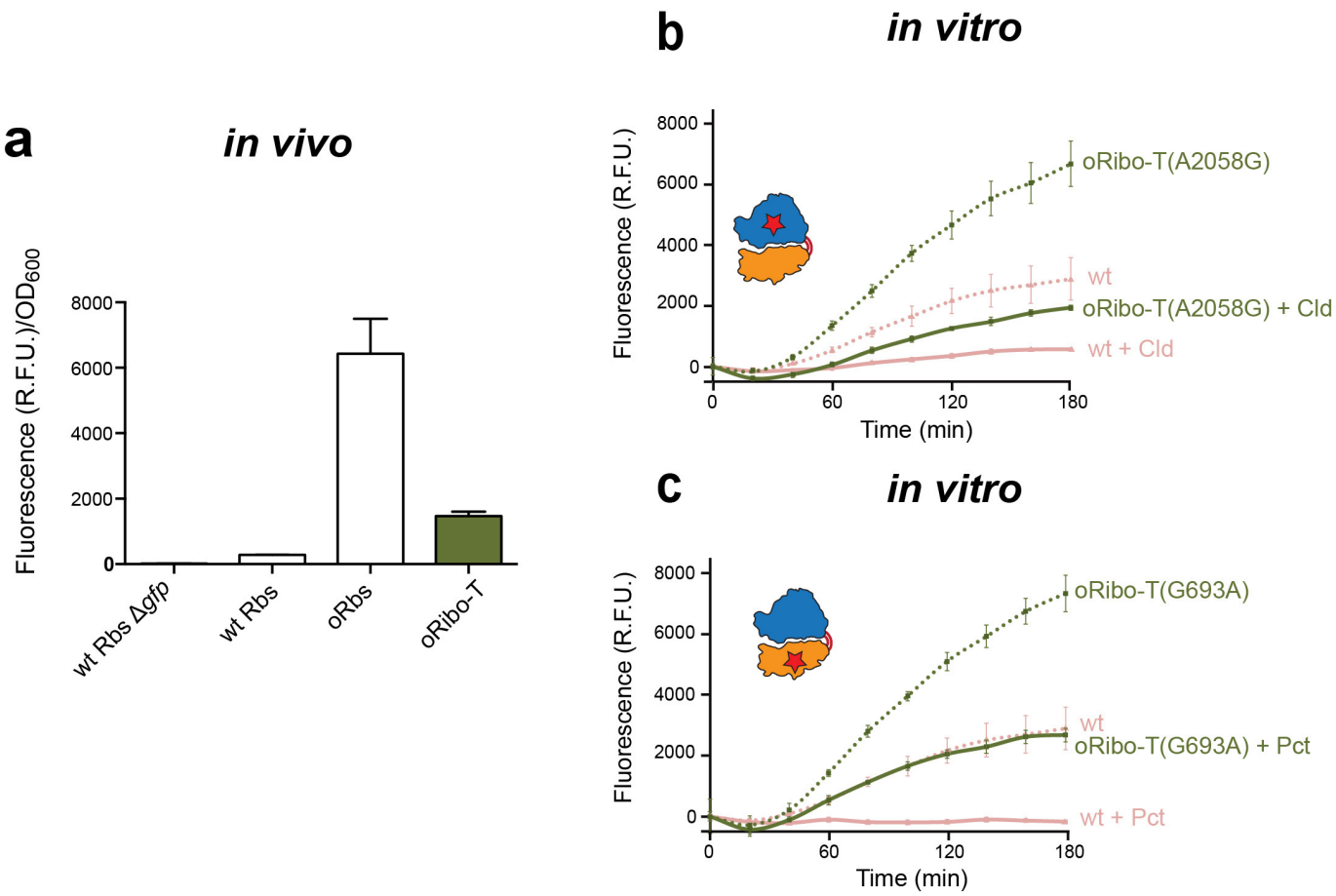

Extended Data Figure 8 | Translation of the orthogonal *sf-gfp* gene by oRibo-T *in vivo* and *in vitro*. **a**, Expression of an orthogonal *sf-gfp* reporter in the *E. coli* POP2136 cells transformed with pAM552 plasmid encoding wild-type rRNA (wt Rbs), pAM552 with an orthogonal Shine–Dalgarno sequence in 16S rRNA of a non-tethered ribosome (oRbs) or poRibo-T1 expressing an orthogonal Ribo-T (green bar). Cells lacking *gfp* reporter gene (wt Rbs Δgfp) were used as a background fluorescence control. The data represent the average value of six biological replicates in technical triplicates; error bars indicate the s.d. **b**, *In vitro* translation of the orthogonal *sf-gfp* reporter by non-tethered non-orthogonal wt ribosomes (pink lines), or oRibo-T(A2058G) (which also contained cellular wild-type ribosomes) (green lines). The dotted lines correspond to the translation reactions without antibiotic and solid lines represent reactions supplemented with 50 μM clindamycin (Cld). **c**, Same as in **b**, but oRibo-T contained a G693A mutation instead of A2058G and clindamycin was replaced with 100 μM pactamycin (Pct). The red stars indicate the ribosomal subunit carrying the antibiotic-resistance mutation. Graphs in **b** and **c** are each representative of two biological replicates each performed in technical triplicates, and error bars indicating the s.d.

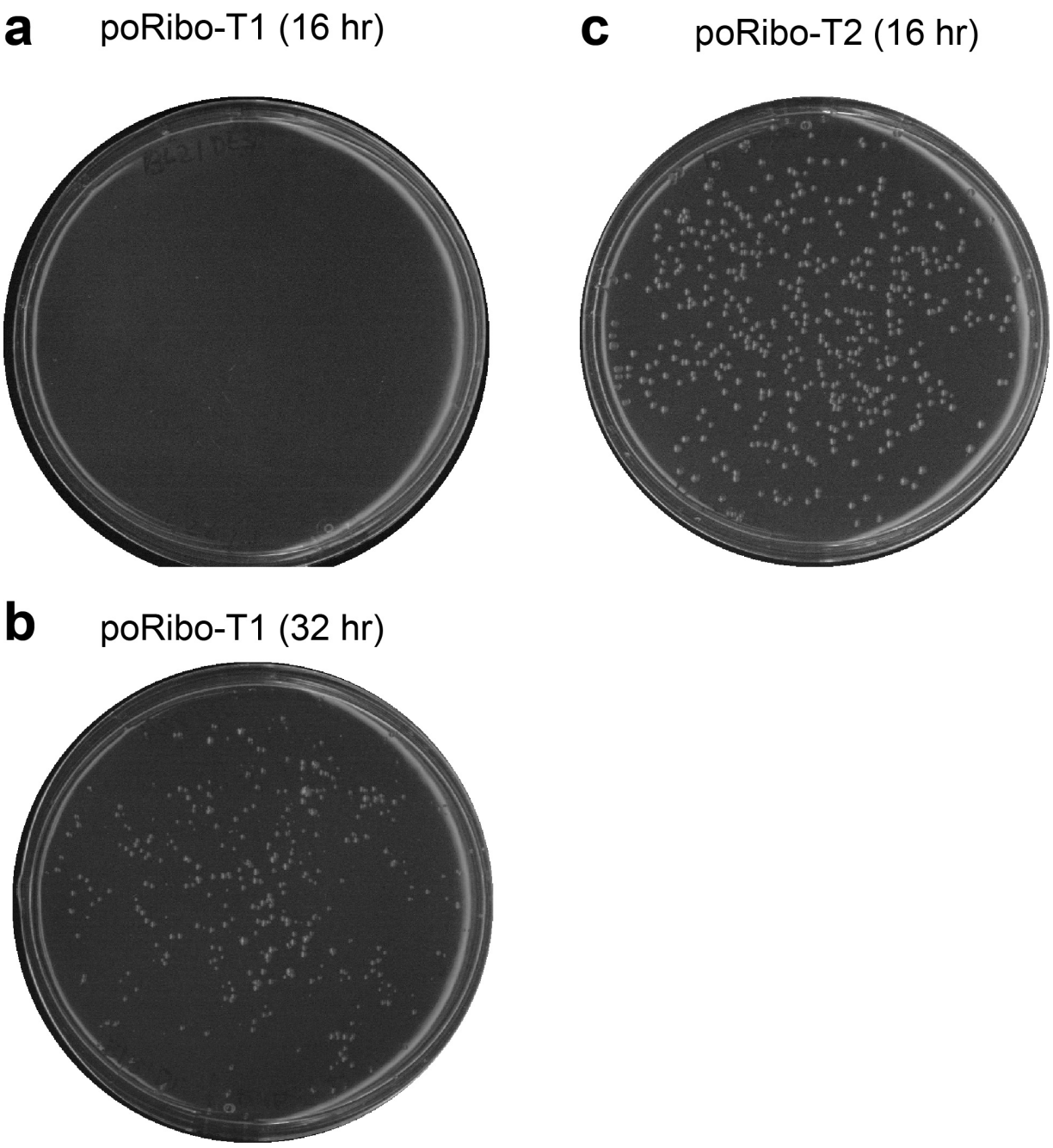

Extended Data Figure 9 | Promoter mutation in oRibo-T improves transformation of the *E. coli* cells. **a**, **b**, Several *E. coli* strains, including BL21 shown in this figure, as well as JM109 and C41, produced slowly growing, heterogeneous colonies when transformed with poRibo-T1. **c**, Fortuitously, in the course of the experiments we isolated a spontaneous mutant plasmid, poRibo-T2, which showed improved transformation efficiency, producing evenly sized colonies after a single overnight incubation. Sequencing of poRibo-T2 revealed a single mutation in the P_L promoter controlling Ribo-T expression, altering the '-10' box from GATACT to TATACT bringing it closer to the TATAAT consensus. It is unclear why the promoter mutation improves performance of poRibo-T (as well as of non-orthogonal pRibo-T) in 'unselected' *E. coli* cells. The plates show representative results of three independent biological experiments.

Extended Data Table 1 | Characterization of the growth of *E. coli* SQ171 cells expressing a pure population of ribosomes with circularly permuted 23S rRNA

	Doubling time (min) *		Cell density (OD_{600}) at saturation†		
	30 °C	37 °C	30 °C	37 °C	n ¶
pAM552 ‡	61.0 ± 3.2	53.9 ± 1.0	1.04 ± 0.06	0.93 ± 0.03	4
pAM552-AflII §	67.4 ± 1.0	53.3 ± 2.4	1.07 ± 0.01	0.97 ± 0.00	4
CP67 ||	106.4 ± 5.4	69.6 ± 2.1	0.83 ± 0.05	0.41 ± 0.07	3
CP95	144.9 ± 35.9	82.4 ± 24.4	0.66 ± 0.31	0.51 ± 0.18	6
CP104	90.8 ± 10.3	52.7 ± 3.2	0.98 ± 0.03	0.95 ± 0.02	3
CP168	123.8 ± 27.9	57.7 ± 1.9	0.70 ± 0.22	0.88 ± 0.12	10
CP281	100.1 ± 11.0	54.6 ± 10.1	1.01 ± 0.04	0.93 ± 0.13	3
CP549	101.7 ± 18.2	46.5 ± 3.9	1.00 ± 0.02	0.98 ± 0.03	3
CP617	231.7 ± 20.5	91.5 ± 18.5	0.16 ± 0.03	0.85 ± 0.05	4
CP634	162.0 ± 34.2	212.5 ± 58.1	0.46 ± 0.19	0.50 ± 0.10	3
CP879	106.6 ± 4.7	51.4 ± 4.6	1.03 ± 0.02	0.99 ± 0.04	3
CP891	144.5 ± 41.8	60.7 ± 4.1	0.56 ± 0.43	0.76 ± 0.23	6
CP1112	89.6 ± 6.0	57.8 ± 12.2	0.96 ± 0.02	0.91 ± 0.12	3
CP1178	102.5 ± 11.0	46.2 ± 1.3	0.96 ± 0.02	0.99 ± 0.01	3
CP1498	167.5 ± 17.5	118.0 ± 17.1	0.56 ± 0.32	0.52 ± 0.19	3
CP1511	131.5 ± 4.2	76.7 ± 1.5	0.88 ± 0.01	0.88 ± 0.01	3
CP1587	98.1 ± 12.4	55.1 ± 6.6	0.93 ± 0.05	0.92 ± 0.08	3
CP1716	174.4 ± 31.9	117.8 ± 16.5	0.44 ± 0.16	0.62 ± 0.34	3
CP1733	117.3 ± 8.2	83.8 ± 2.2	0.95 ± 0.01	0.80 ± 0.01	3
CP1741	230.0 ± 14.7	269.0 ± 50.3	0.28 ± 0.00	0.66 ± 0.09	3
CP1873	108.4 ± 6.5	52.9 ± 0.8	0.94 ± 0.01	0.91 ± 0.01	3
CP2148	83.0 ± 2.9	52.4 ± 3.9	0.73 ± 0.09	0.82 ± 0.02	4
CP2800	85.9 ± 15.7	53.5 ± 9.7	1.04 ± 0.03	0.91 ± 0.12	3
CP2861	138.4 ± 10.7	93.7 ± 4.5	0.88 ± 0.00	0.83 ± 0.04	3

*Growth in 100 μl LB media supplemented with 50 μg ml^{-1} carbenicillin in 96-well plate with shaking.
†After 18 h of growth.
‡pAM552: wild-type *rrnB* operon.
§pAM552-AflII: *rrnB* operon with the 23S rRNA mutations G2C and C2901G used to introduce the AflII restriction sites.
||CPx: *rrnB* with 23S circular permutations and G2C/C2901G mutations; x indicates the 5′ starting nucleotide of the circularly permuted 23S gene.
¶Biological replicates are indicated in the '*n*' column, which is the number of separate colonies that were used for each mean number and s.d.